Leading Λ Production at the Electron-Ion Collider

Fernando Navarra

University of São Paulo USP

with Gonçalves, Spiering, Carvalho, Khemchandani, Martínez Torres

Physics Opportunities at an Electron-Ion Collider 2023

FAPESP ICTP unesp IFT - UNESP PRINCIPIA Jefferson Lab Brookhaven National Laboratory I·ANQCD

May 2-6, 2023 (Tuesday – Saturday)

ICTP-SAIFR, São Paulo, Brazil

Principia Institute

Tagged Deep Inelastic Scattering (TDIS)

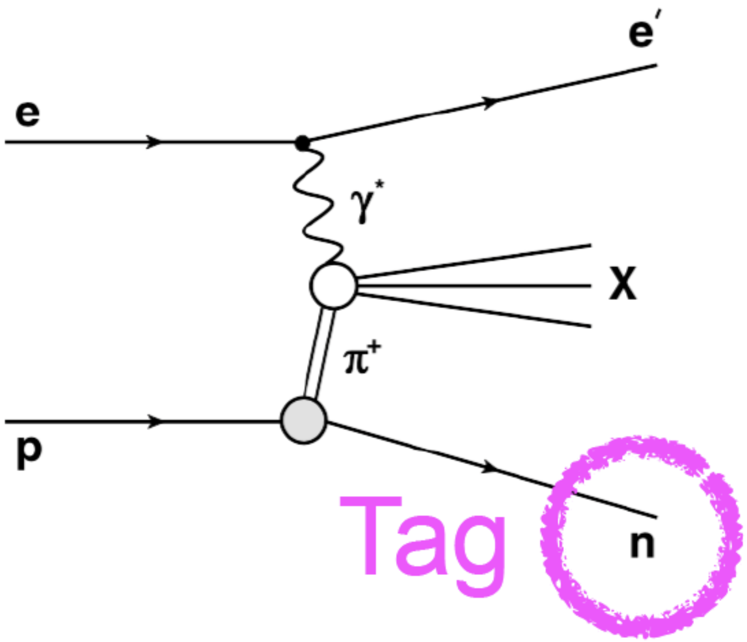

Leading Neutron

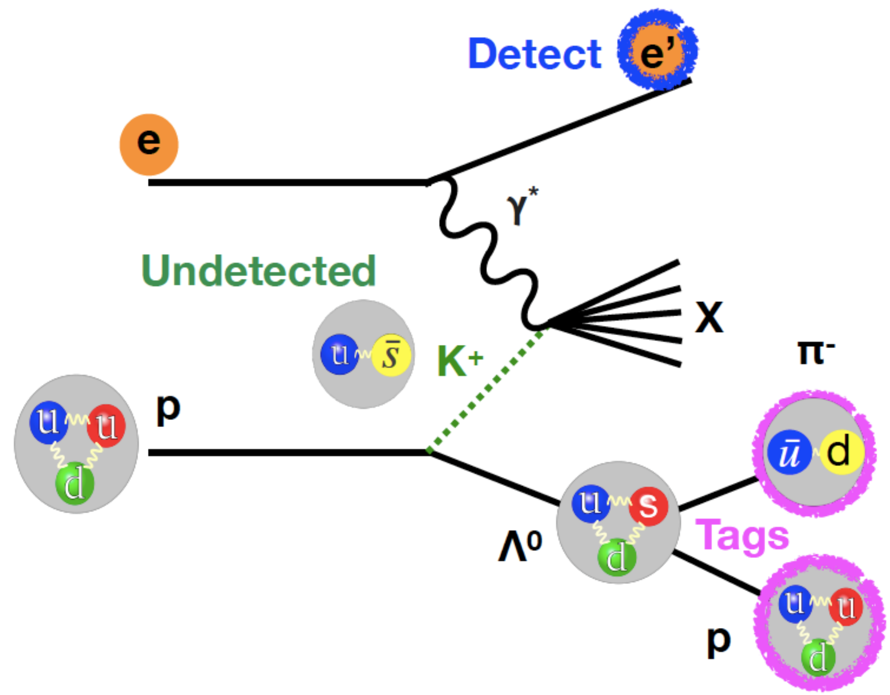

Leading Lambda

Main goal: study the structure of pions and kaons !

Leading versus non-leading neutrons in DIS

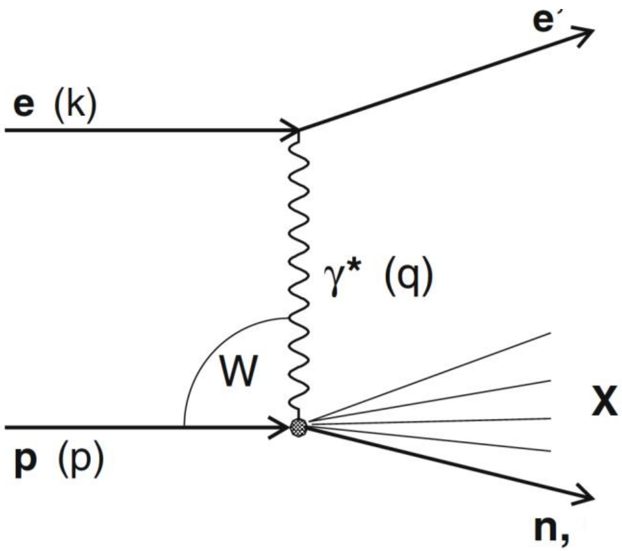

standard DIS

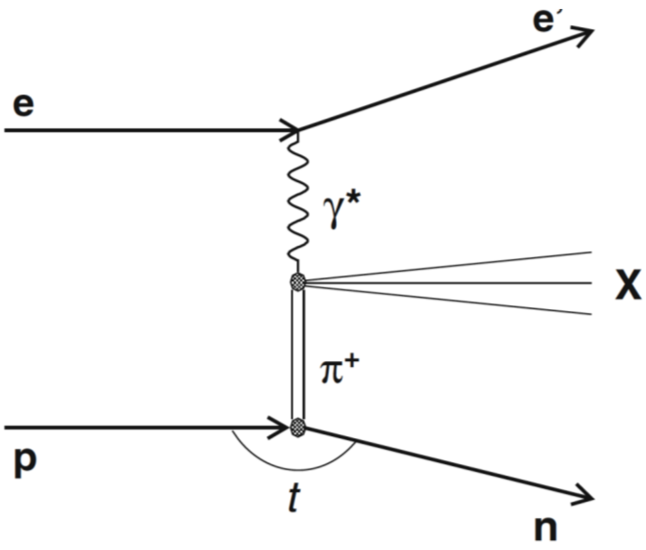

Sullivan process

How important is the Sullivan process ?

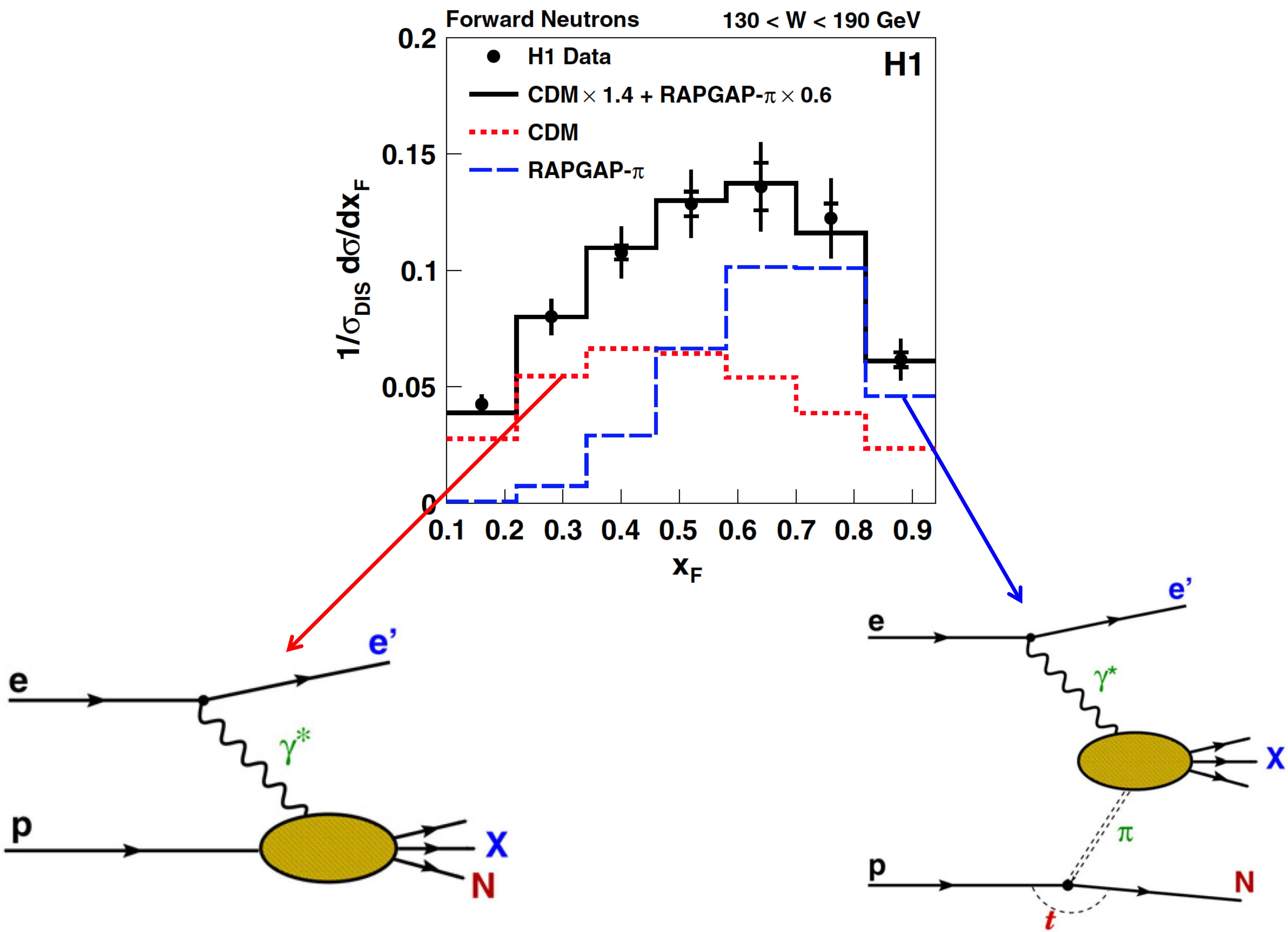

Forward Neutrons
130 < W < 190 GeV
H1 Data
CDM × 1.4 + RAPGAP-π × 0.6
CDM
RAPGAP-π
H1
$1/\sigma_{DIS}\, d\sigma/dx_F$
x_F
0.2
0.15
0.1
0.05
0
0.1 0.2 0.3 0.4 0.5 0.6 0.7 0.8 0.9
e
e'
γ^*
p
X
N
π
t

We need the Sullivan process ("pion cloud") !

A.W. Thomas, Phys. Lett. 126B, 97-100 (1983).

In a 1983 paper, Thomas commented that "...it is rather disturbing that no one has yet provided direct experimental evidence of a pionic component in the nucleon"

In particular, it was predicted that the nucleon sea should have an up/down sea-quark flavor asymmetry

ubar/dbar asymmetry in the nucleon sea

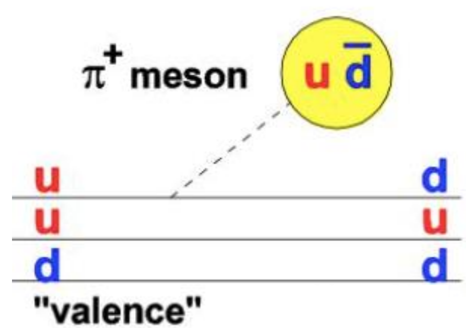

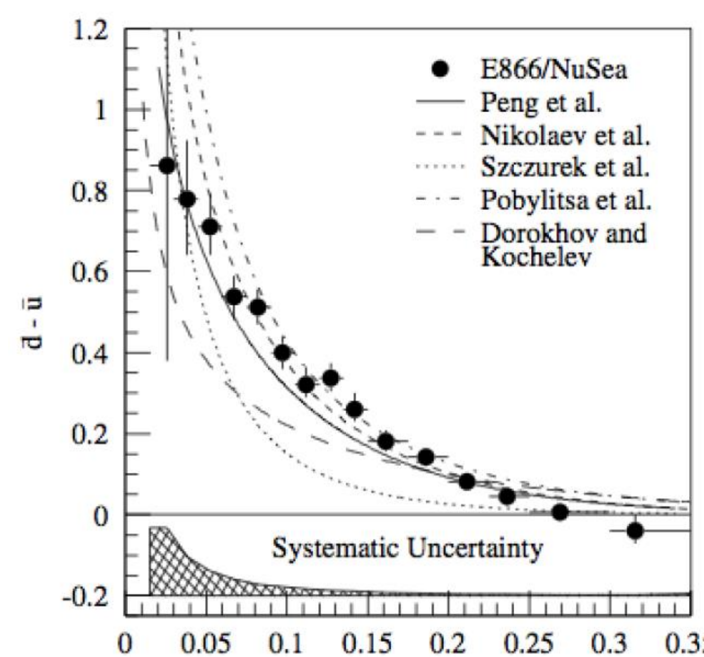

arXiv:1907.08218

This talk

- Discuss the pion vertex
- Pion-photon in the color dipole approach (gluon saturation effects)
- Absorption Effects
- Inclusive and exclusive processes (understand HERA data)

$$e^- + p \to e^- + X + n$$

$$e^- + p \to e^- + \rho^0 + \pi^+ + n$$

- Extension to Proton-Proton
- Extension to Leading Lambda

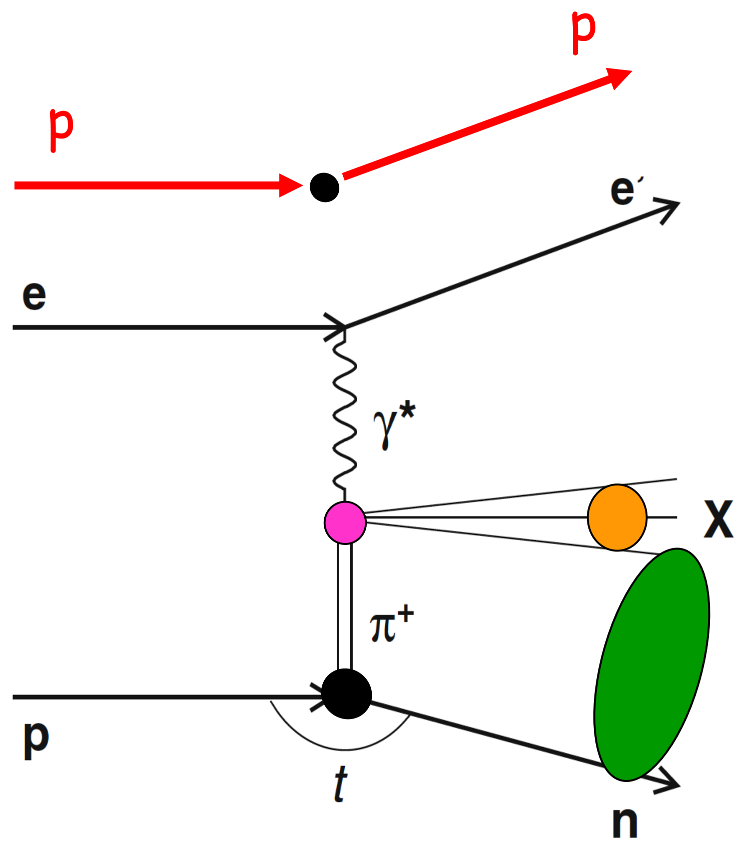

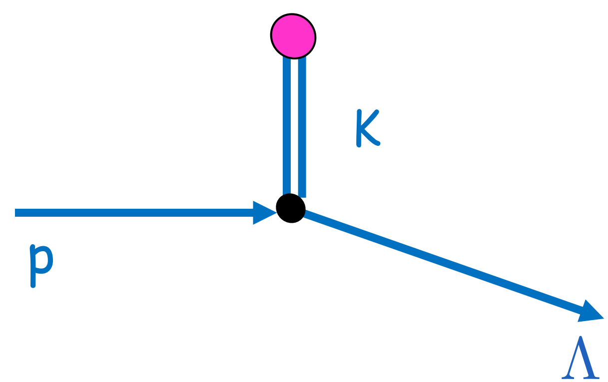

$$\boxed{e^- + p \rightarrow e^- + X + n}$$

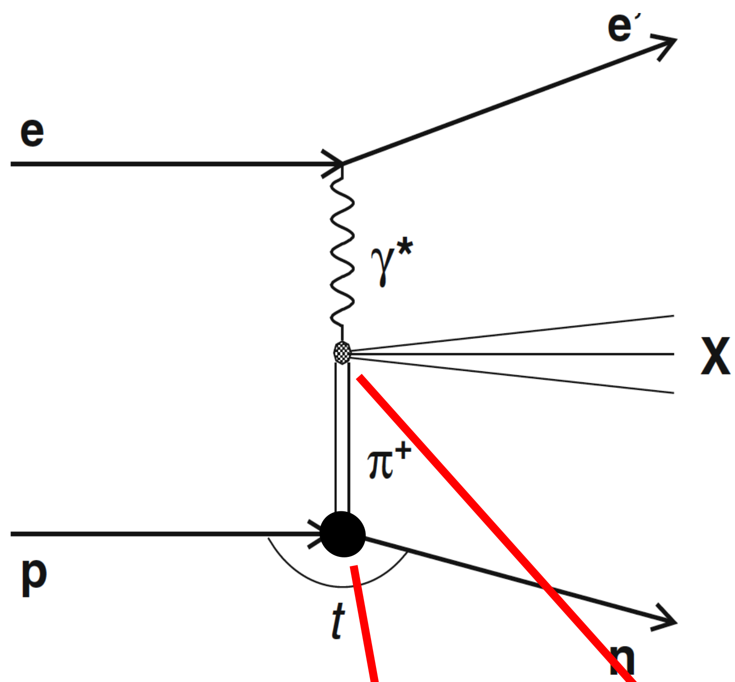

$$\frac{d^2\sigma(W, Q^2, x_L, t)}{dx_L dt} = \underbrace{f_{\pi/p}(x_L, t)}_{\text{Splitting function}}\underbrace{\sigma_{\gamma^*\pi}(\hat{W}^2, Q^2)}_{\text{Photon-pion cross section}}$$

Pion splitting function

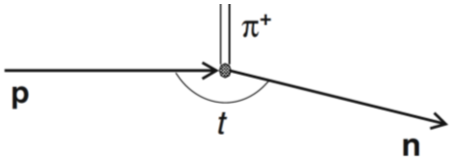

$$f_{\pi/p}(x_L,t) = \frac{1}{4\pi}\frac{2g^2_{p\pi p}}{4\pi}\frac{-t}{(t-m_\pi^2)^2}(1-x_L)^{1-2\alpha(t)}[F(x_L,t)]^2$$

Form factors:

$F_1(x_L,t) = exp[R^2\frac{(t-m_\pi^2)}{(1-x_L)}]$ $\alpha(t)=0$ light cone

$F_2(x_L,t) = 1$ $\alpha(t)=\alpha_\pi(t)=t$

$F_3(x_L,t) = exp[b(t-m_\pi^2)]$ $\alpha(t)=\alpha_\pi(t)=t$ reggeized pion

$F_4(x_L,t) = \frac{(\Lambda^2-m_\pi^2)}{(\Lambda^2-t^2)}$ $\alpha(t)=0$ monopole

$F_5(x_L,t) = [\frac{(\Lambda^2-m_\pi^2)}{(\Lambda^2-t^2)}]^2$ $\alpha(t)=0$ dipole

Carvalho, Gonçalves, Spiering, FSN, PLB 752 (2016) 76

Kopeliovich, Potashnikova, Povh,Schmidt, PRD (2012)

Can we replace the form factors by something better ?

Replace $\mathcal{L}^{\mathrm{PS}}_{\pi N} = -g_{\pi NN}\bar{\psi}_N i\gamma_5 \boldsymbol{\tau}\cdot\boldsymbol{\pi}\psi_N,$ by a Chiral Effective Lagrangian :

$$\mathcal{L}_{\pi N} = \frac{g_A}{2f_\pi}\bar{\psi}_N\gamma^\mu\gamma_5\,\boldsymbol{\tau}\cdot\partial_\mu\boldsymbol{\pi}\,\psi_N - \frac{1}{(2f_\pi)^2}\bar{\psi}_N\gamma^\mu\,\boldsymbol{\tau}\cdot(\boldsymbol{\pi}\times\partial_\mu\boldsymbol{\pi})\,\psi_N$$

M. Burkardt, K. S. Hendricks, C. R. Ji, W. Melnitchouk and A. W. Thomas, Phys. Rev. D **87**, 056009 (2013)

Y. Salamu, C. R. Ji, W. Melnitchouk and P. Wang, Phys. Rev. Lett. **114**, 122001 (2015)

$$f_6(x_L) = f_{\pi/p}(y) = \frac{g_A^2 m_n^2}{(4\pi f_\pi)^2}\int_0^{\Lambda_c^2} dp_T^2\,\frac{y(p_T^2+y^2m_n^2)}{[p_T^2+y^2m_n^2+(1-y)m_\pi^2]^2}$$

$\Lambda_c = 0.2$ GeV

$y = 1 - x_L$

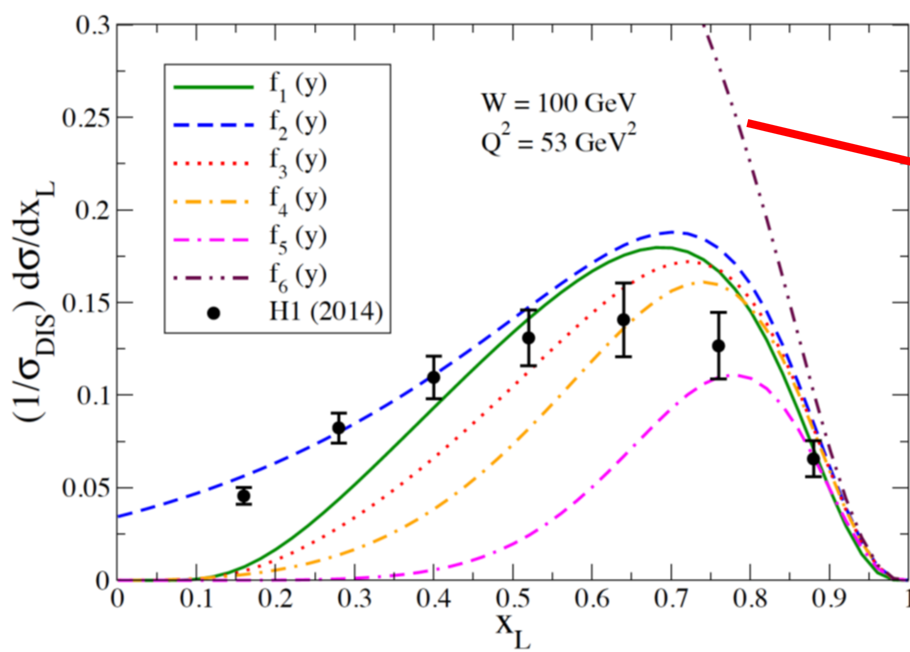

(Psycho)

No chiral theory for kaon emission...

Pion-photon cross section in the dipole approach

$$\frac{d^2\sigma(W,Q^2,x_L,t)}{dx_L dt} = f_{\pi/p}(x_L,t)\sigma_{\gamma^*\pi}(\hat{W}^2,Q^2)$$

Very high energies : LeHC

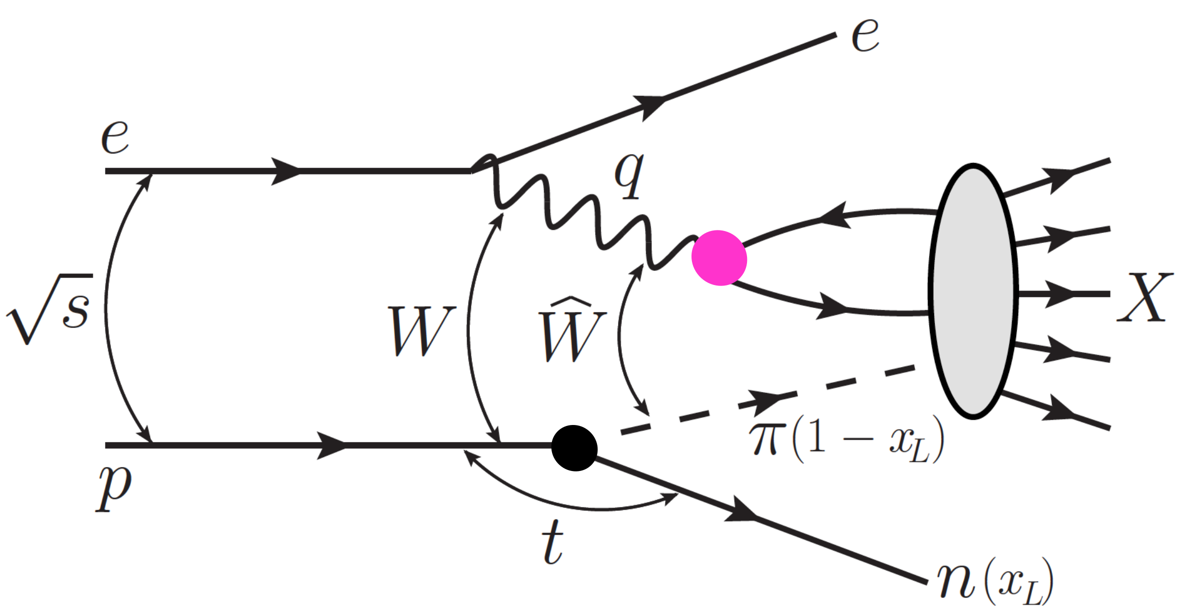

$$\hat{W}^2 = (1-x_L)\,W^2$$

$$\hat{x} = \frac{Q^2+m_f^2}{\hat{W}^2+Q^2}$$

Pion-photon cross section in the dipole approach

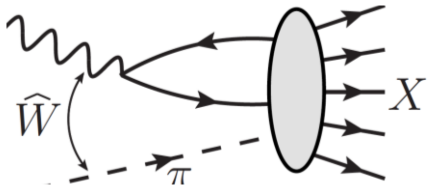

$$\sigma_{\gamma^*\pi}(\hat{x}, Q^2) = \int_0^1 dz \int d^2r \sum_{L,T} |\Psi_{L,T}(z, r, Q^2)|^2 \, \sigma_{d\pi}(\hat{x}, r)$$

Photon wave function:

$$\begin{cases} |\psi_L(z,r)|^2 = \dfrac{3\alpha_{em}}{\pi^2} \displaystyle\sum_f e_f^2 4Q^2 z^2 (1-z)^2 K_0^2(\epsilon r) \\ |\psi_T(z,r)|^2 = \dfrac{3\alpha_{em}}{2\pi^2} \displaystyle\sum_f e_f^2 \left\{ [z^2 + (1-z^2] \epsilon^2 K_1^2(\epsilon r) + m_f^2 K_0^2(\epsilon r) \right\} \end{cases}$$

$$\epsilon^2 = z(1-z)Q^2 + m_f^2$$

Dipole-pion cross section:

$$\sigma_{d\pi}(\hat{x}, r) = 2 \int d^2b \, \mathcal{N}_\pi(\hat{x}, r, b) = \sigma_0 \, \mathcal{N}_\pi(\hat{x}, r)$$

$$\mathcal{N}_\pi(\hat{x}, r, b) = R_q \, \mathcal{N}_p(\hat{x}, r, b)$$

$$\sigma_{d\pi} = \frac{2}{3} \sigma_{dp}$$

(aditive quark model)

$$R_q = \frac{2}{3}$$

Dipole-proton amplitude

Non-linear (saturation) models:

$$\mathcal{N}(r,\hat{x}) = [1 - exp(-\frac{(Q_s(\hat{x})r)^2}{4})]$$

GBW

$$N(r,\hat{x}) = \begin{cases} \mathcal{N}_0 \left(\frac{r_, Q_s}{2}\right)^{2\left(\gamma_s + \frac{\ln(2/rQ_s)}{\kappa\,\lambda\,Y}\right)}, & \text{for } rQ_s(\hat{x}) \le 2 \\ 1 - \exp^{-a\,\ln^2(b\,r\,Q_s)}, & \text{for } rQ_s(\hat{x}) > 2 \end{cases}$$

IIM-S

$$Q_s^2(\hat{x}) = Q_0^2\left(\frac{x_0}{\hat{x}}\right)^{\lambda} \qquad \hat{x} = \frac{Q^2 + m_f^2}{\hat{W}^2 + Q^2}$$

Linear (no saturation) model:

$$\sigma_{dip}(r,\hat{x}) = \frac{\pi^2}{3} r^2 \alpha_s \hat{x} g(x, 10/r^2)$$

Blättel, Baym, Frankfurt, Heiselberg, Strikman, PRD (1993)

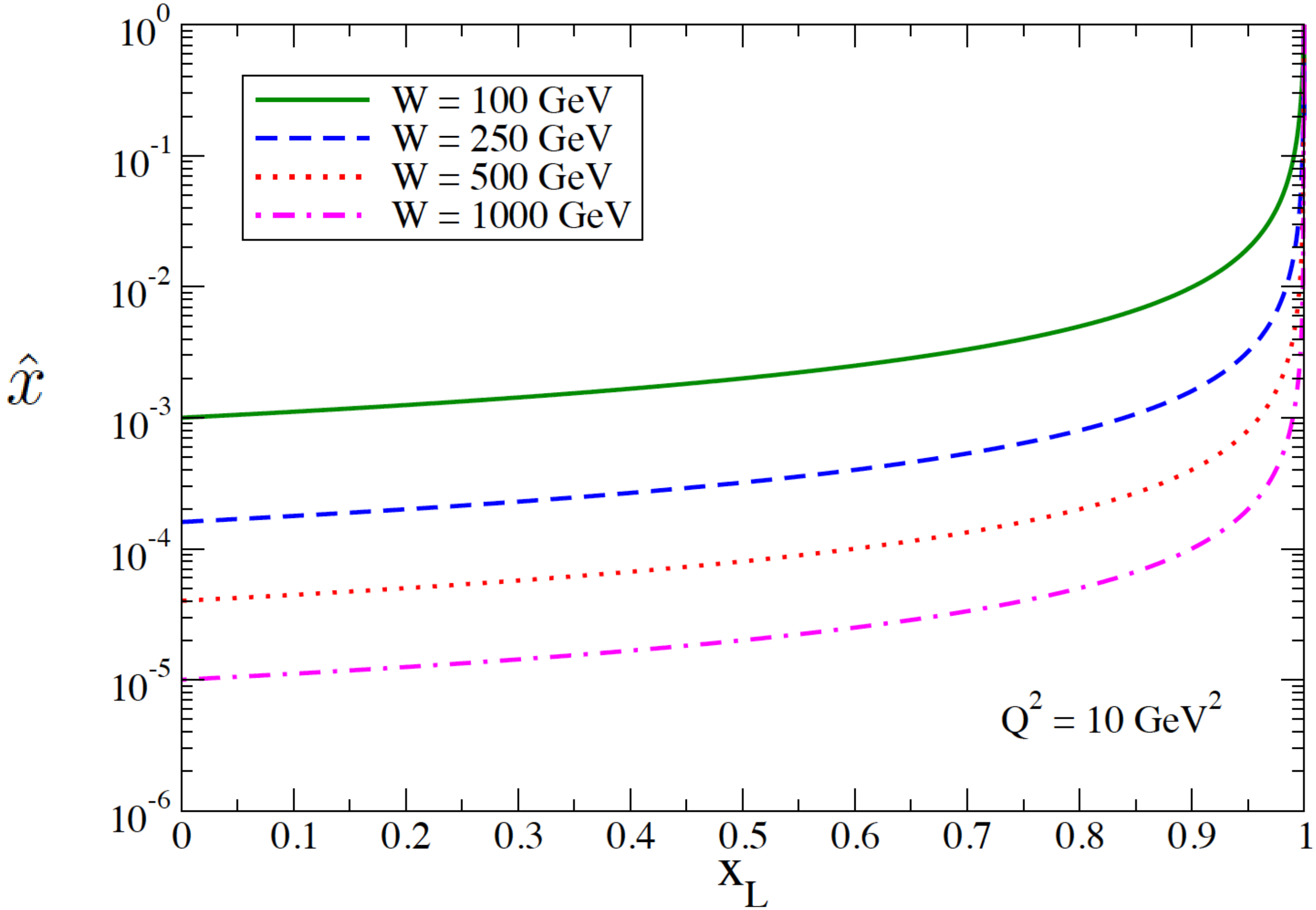

$$\hat{x} = \frac{Q^2 + m_f^2}{\hat{W}^2 + Q^2} = \frac{Q^2 + m_f^2}{(1 - x_L)W^2 + Q^2}$$

Leading neutron/Lambda production
can be low x physics !

Absorption Effects I

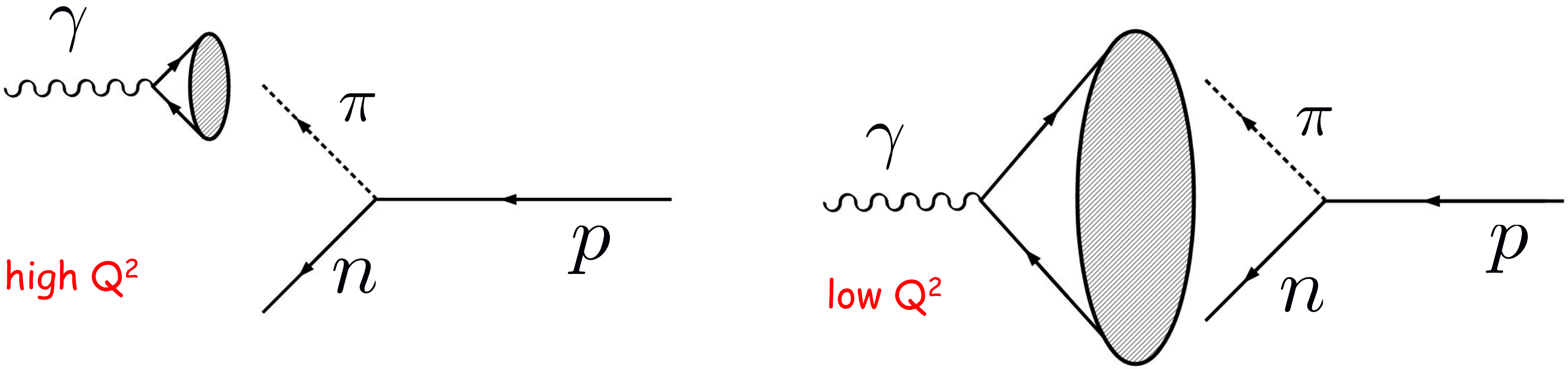

Survival probability

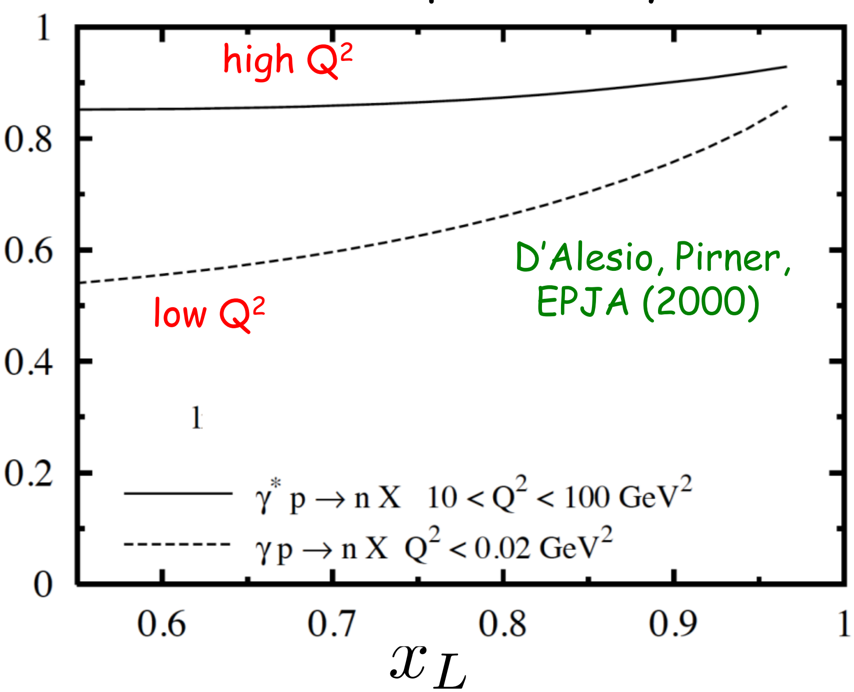

Approximated by a constant factor :

$$\frac{d\sigma}{dx_L} = K \; f_{\pi/p}(x_L, t)\sigma_{\gamma^*\pi}(\hat{W}^2, Q^2)$$

Kopeliovich, Potashnikova, Povh, Schmidt, PRD (2012)

H1: V. Andreev et al., EJPC 76, 41 (2016)

HERA Data

$$e^- + p \to e^- + X + n$$

Aditive quark model : $R_q = \frac{2}{3}$

No absorption : $K = 1$

$$\sigma_{DIS} = \frac{4\pi^2 \alpha_{em}}{Q^2} \frac{c}{x^\beta}$$

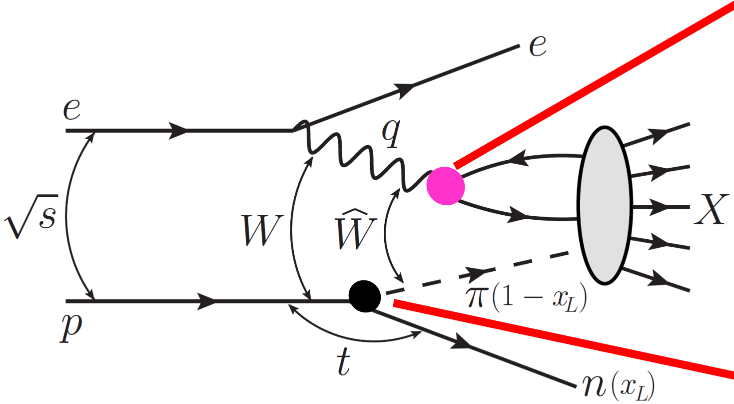

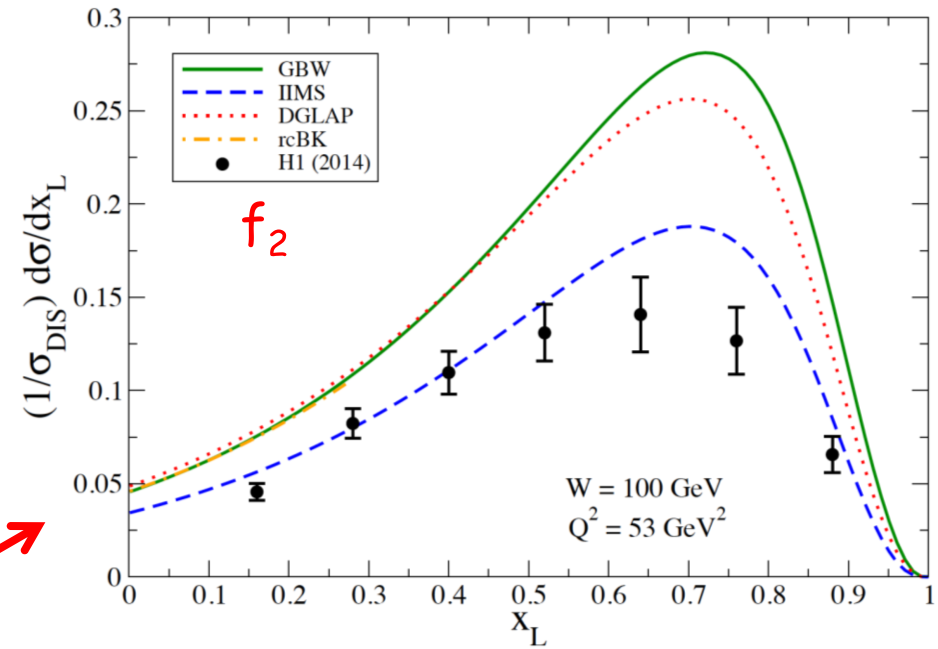

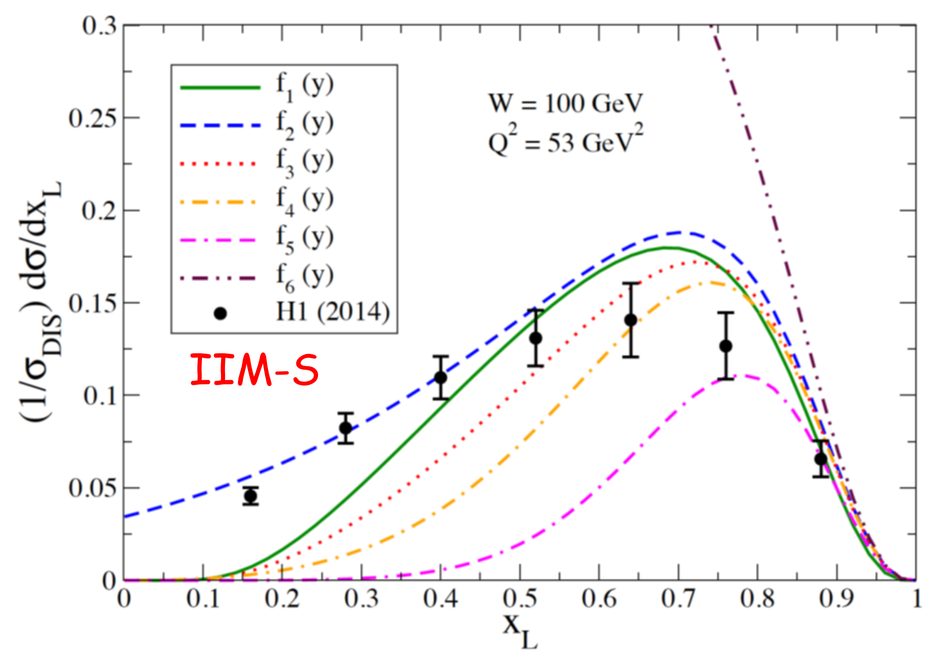

Keep the blue line and include absorption !

Absorption :

Energy Dependence

$K = 0.7$

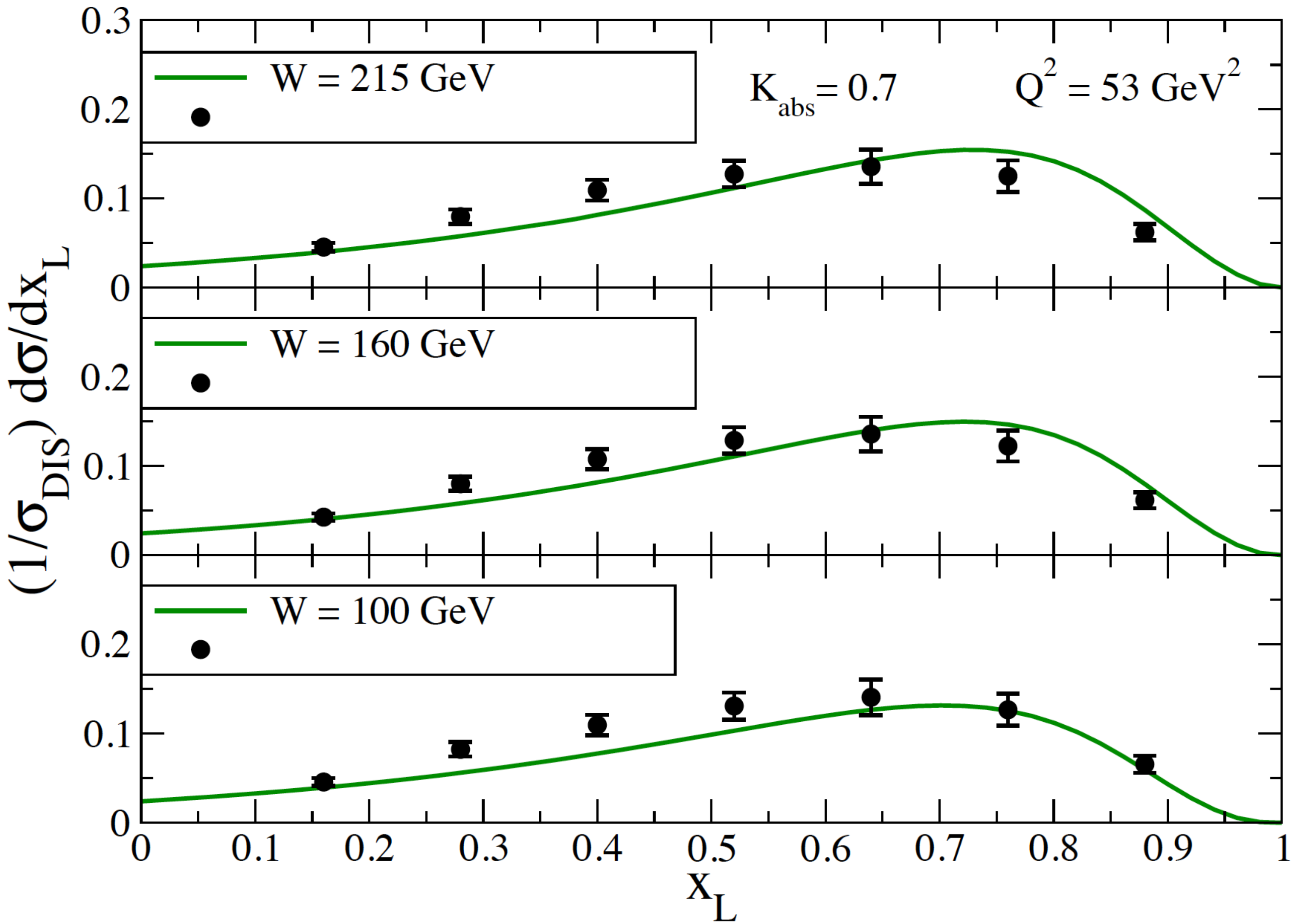

Carvalho, Gonçalves, Spiering, FSN, PLB 752 (2016) 76

Prediction: "Feynman scaling"

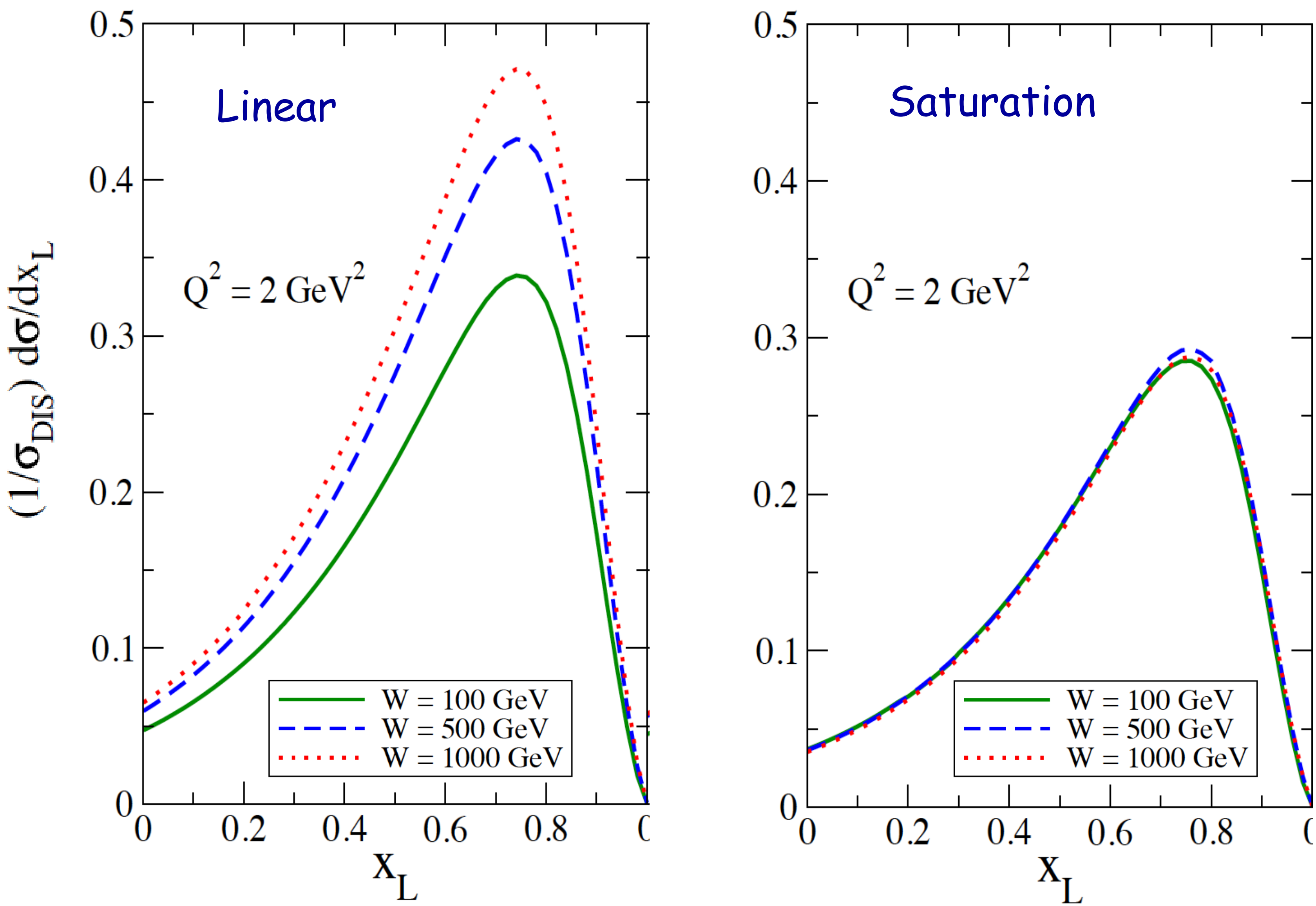

$$e^- + p \to e^- + \rho^0 + \pi^+ + n$$

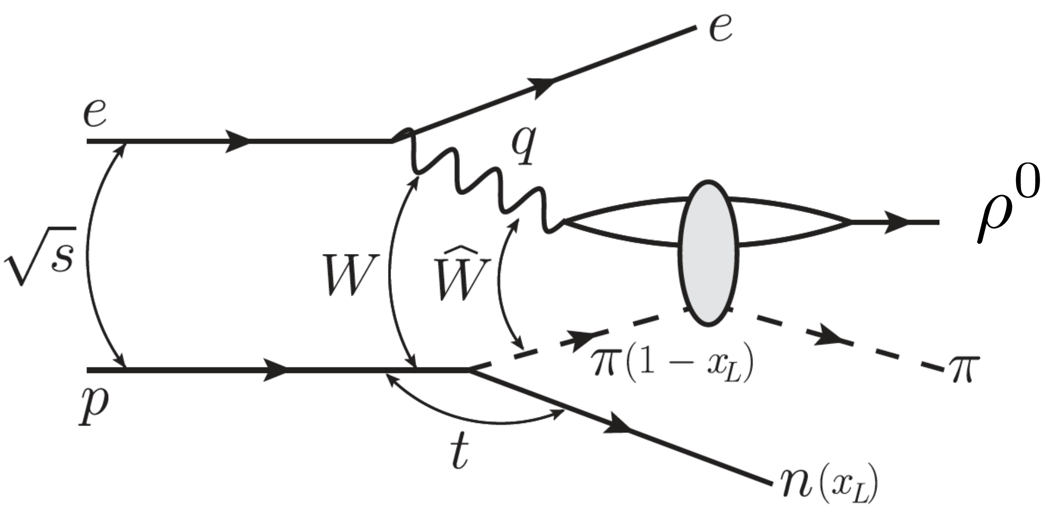

"Tag" of an event with a large dipole !

Expect stronger absorption !

$$\frac{d^2\sigma(W,Q^2,x_L,t)}{dx_L dt} = K \; f_{\pi/p}(x_L,t)\sigma_{\gamma^*\pi}(\hat{W}^2,Q^2)$$

$$\sigma(\gamma^*\pi \to E\pi) = \sum_{i=L,T} \int_{-\infty}^{0} \frac{d\sigma_i}{d\hat{t}} d\hat{t} = \frac{1}{16\pi} \sum_{i=L,T} \int_{-\infty}^{0} |\mathcal{A}_i^{\gamma^*\pi\to E\pi}(x,\Delta)|^2 d\hat{t}$$

$$\mathcal{A}_{T,L}^{\gamma^*\pi\to E\pi}(\hat{x},\Delta) = i\int dz d^2\boldsymbol{r} d^2\boldsymbol{b} e^{-i[\boldsymbol{b}-(1-z)\boldsymbol{r}].\boldsymbol{\Delta}} \; (\Psi^{E*}\Psi)_{T,L} 2\mathcal{N}_\pi(\hat{x},\boldsymbol{r},\boldsymbol{b})$$

Vector meson wave function

Photon wave function

Scattering amplitude

$$\begin{cases} (\Psi_V^*\Psi)_T = \dfrac{\hat{e}_f e}{4\pi}\dfrac{N_c}{\pi z(1-z)}\{m_f^2 K_0(\epsilon r)\phi_T(r,z) \; - [z^2+(1-z)^2]\epsilon K_1(\epsilon r)\partial_r\phi_T(r,z)\} \\ (\Psi_V^*\Psi)_L = \dfrac{\hat{e}_f e}{4\pi}\dfrac{N_c}{\pi} 2Qz(1-z)K_0(\epsilon r)\left[M_V\phi_L(r,z) + \delta\dfrac{m_f^2-\nabla_r^2}{M_V z(1-z)}\phi_L(r,z)\right] \end{cases}$$

Boosted Gaussian

$$\phi_{T,L}(r,z) = \mathcal{C}_{T,L} z(1-z)\exp\left[-\frac{m_f^2 R^2}{8z(1-z)} \; -\frac{2z(1-z)r^2}{R^2} + \frac{m_f^2 R^2}{2}\right]$$

Gauss LC

$$\phi_T(r,z) = N_T[z(1-z)]^2\exp\left(-r^2/2R_T^2\right)$$

$$\phi_L(r,z) = N_L z(1-z)\exp\left(-r^2/2R_L^2\right)$$

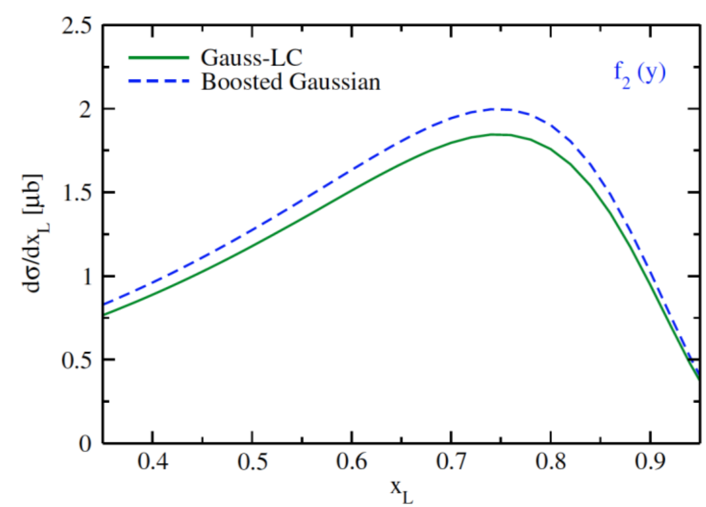

$$e^- + p \to e^- + \rho^0 + \pi^+ + n$$

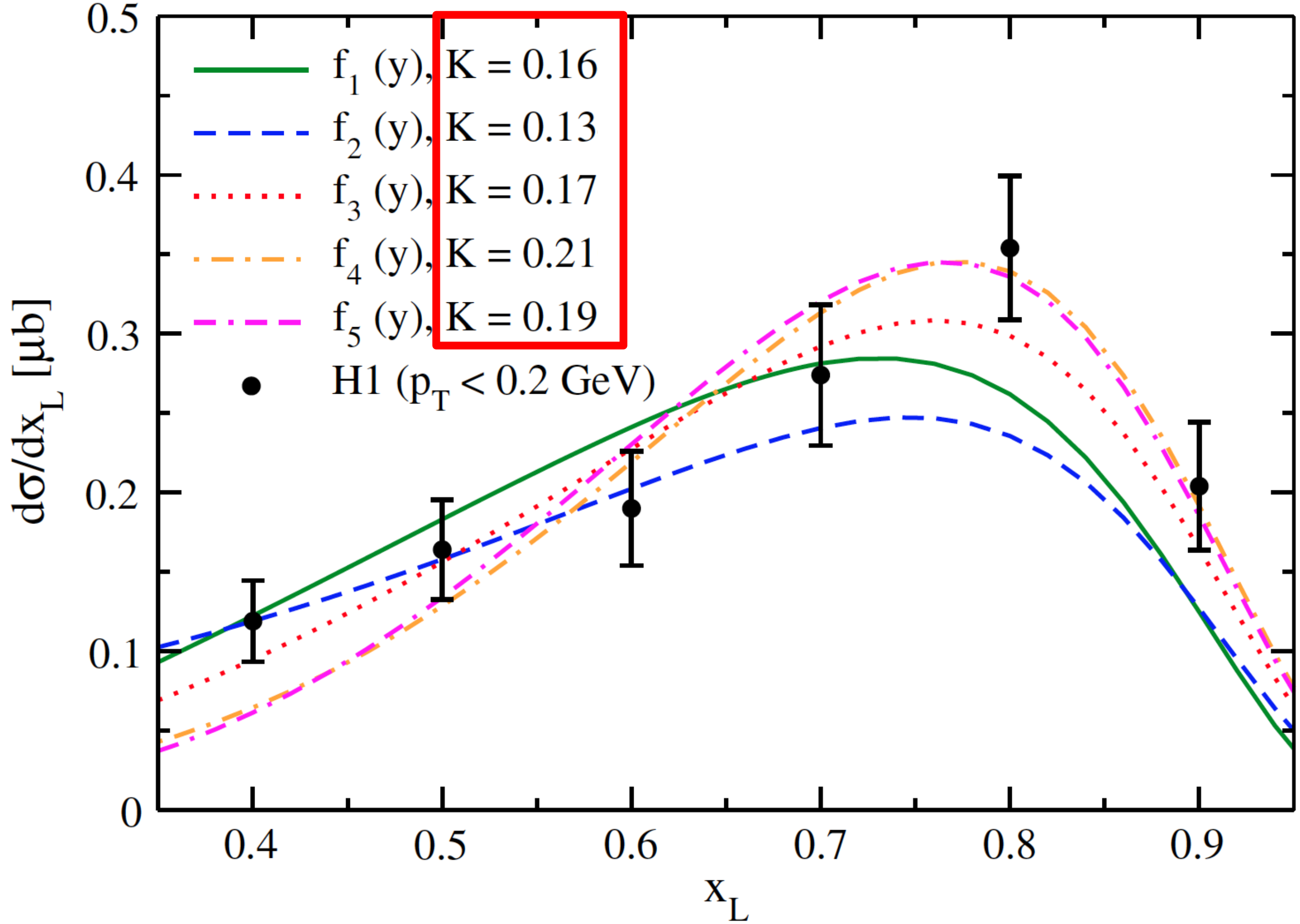

H1: V. Andreev et al., EJPC 76, 41 (2016)

Gonçalves, FSN, Spiering, PRD 93 (2016) 054025

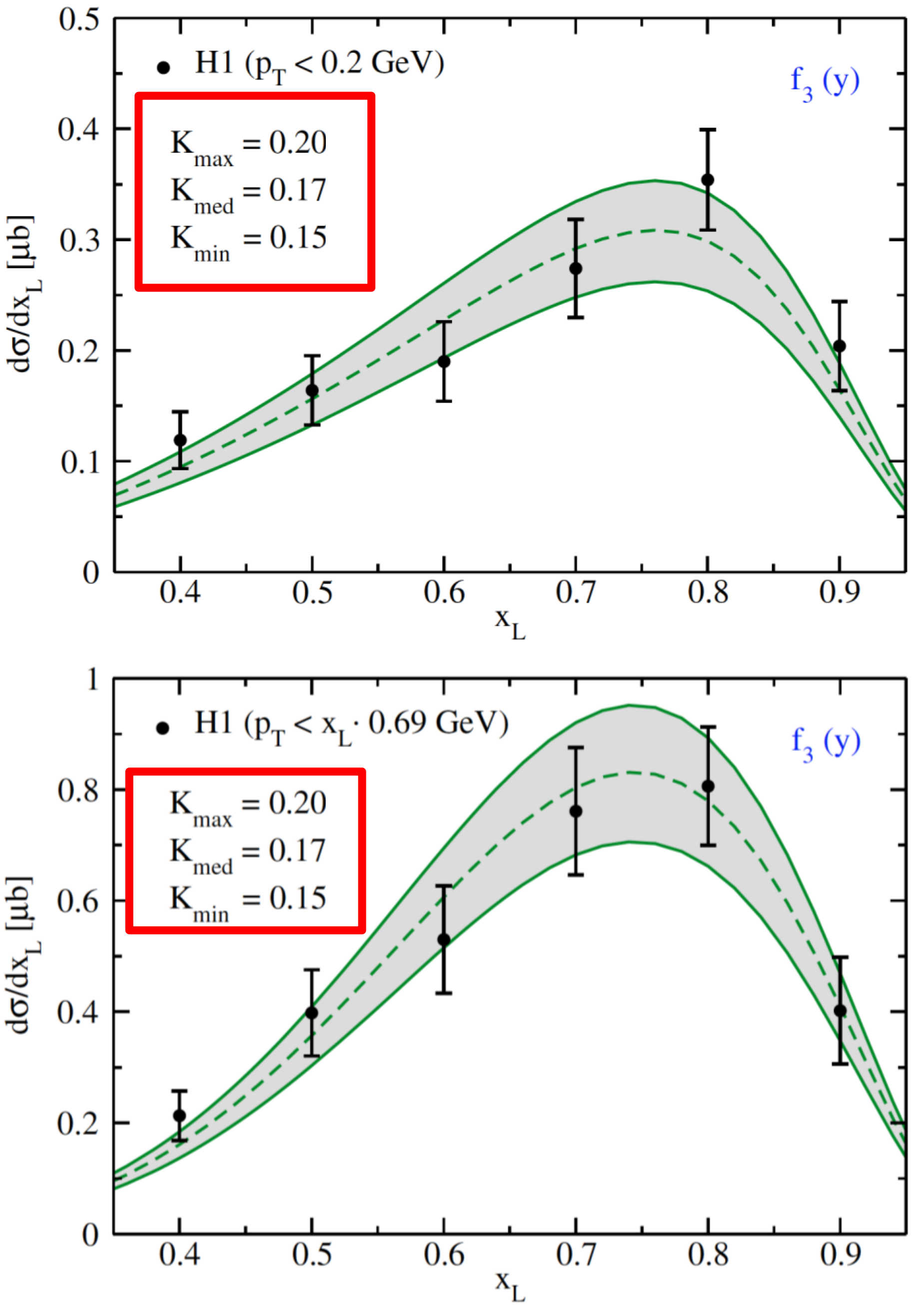

Have to fit
all data points...

We really need absorption !

Straightforward extension to :

$$p + p \to p + \rho^0 + \pi^+ + n$$

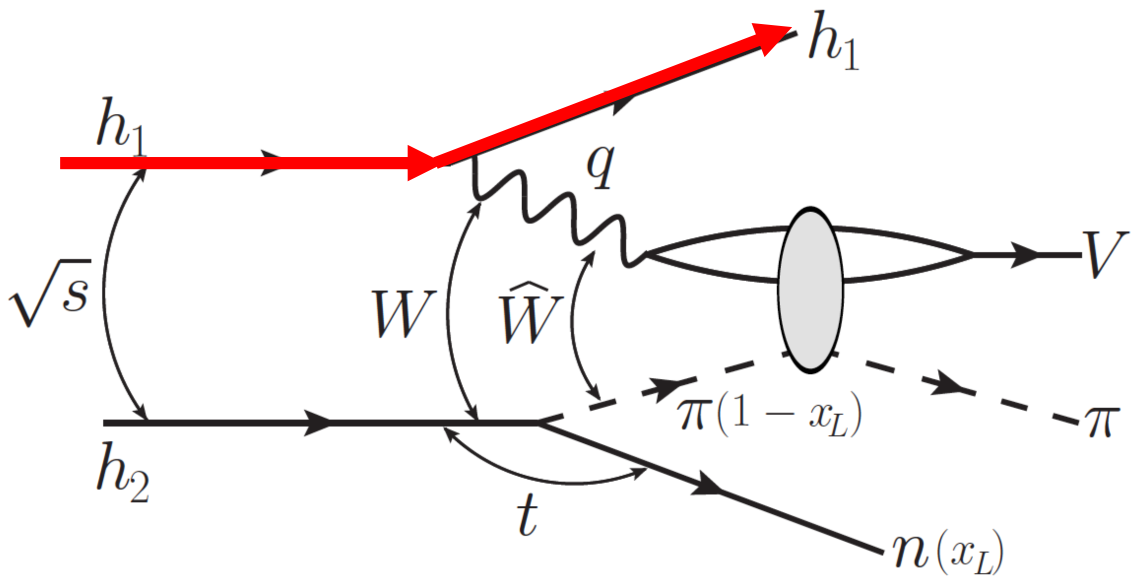

Gonçalves, Moreira, FSN, Spiering, PRD 94 (2016) 014009

Absorption Effects II

No constant factor approximation

Improve dipole-neutron cross section

D'Alesio, Pirner, EPJA (2000)

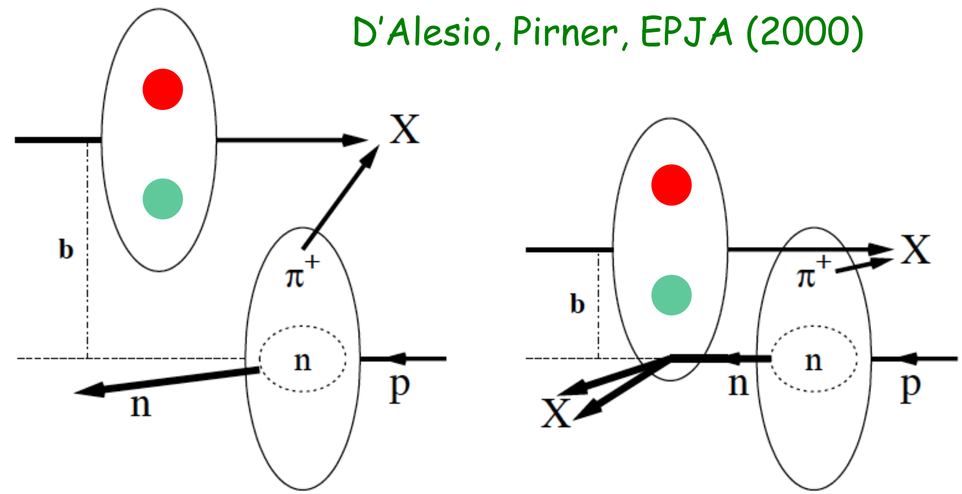

$$\frac{d\sigma(W,Q^2,x_L)}{dx_L} = \int d^2b_{\mathrm{rel}}\rho_{n\pi}(x_L,b_{\mathrm{rel}}) \int dz\, d^2r \sum_{L,T} |\Psi_{T,L}(z,r,Q^2)|^2\, \sigma_{d\pi}(x_\pi,r) S^2_{eik}(r,b_{\mathrm{rel}})$$

$$S^2_{eik}(r,b_{\mathrm{rel}}) = \left\{1 - \Lambda^2_{\mathrm{eff}}\frac{\sigma_{dn}(x_n,r)}{2\pi}\exp\left[-\frac{\Lambda^2_{\mathrm{eff}} b^2_{\mathrm{rel}}}{2}\right]\right\}$$

geometry

$$\Lambda^2_{\mathrm{eff}} = \frac{\Lambda^2_{p\pi}\Lambda^2_{pn}}{\Lambda^2_{p\pi}+\Lambda^2_{pn}}$$

dynamics

$$\sigma_{dn}(x_n,r) = 2\pi R_p^2 \times \begin{cases} \mathcal{N}_0\left(\frac{rQ_s}{2}\right)^{2\left(\gamma_s+\frac{\ln(2/rQ_s)}{K\lambda Y}\right)}, \\ 1-\mathrm{e}^{-a\ln^2(brQ_s)}, \end{cases}$$

IIMS

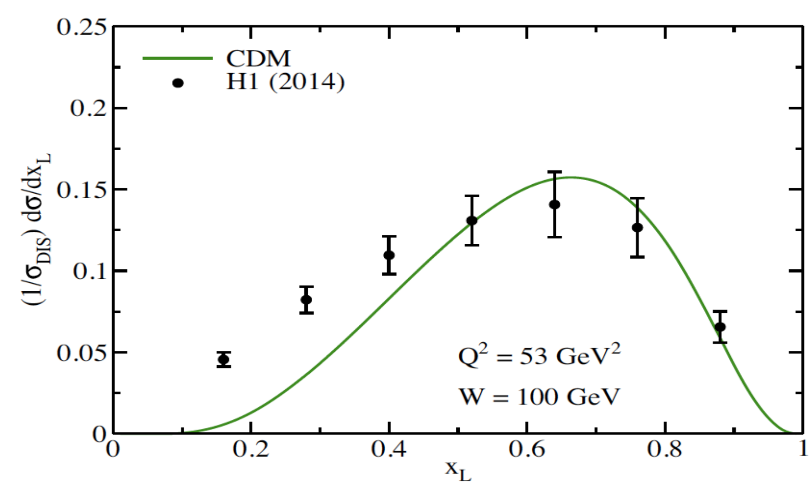

We compute the ratio:

$$K_{abs} = \frac{\frac{d\sigma(W,Q^2,x_L)}{dx_L} = \int d^2 b_{\rm rel} \rho_{n\pi}(x_L, b_{\rm rel}) \int dz\, d^2 r \sum_{L,T} |\Psi_{T,L}(z,r,Q^2)|^2 \;\; \sigma_{d\pi}(x_\pi, r) S^2_{eik}(r, b_{\rm rel})}{\frac{d\sigma(W,Q^2,x_L)}{dx_L} = \int d^2 b_{\rm rel} \rho_{n\pi}(x_L, b_{\rm rel}) \int dz\, d^2 r \sum_{L,T} |\Psi_{T,L}(z,r,Q^2)|^2 \;\; \sigma_{d\pi}(x_\pi, r)}$$

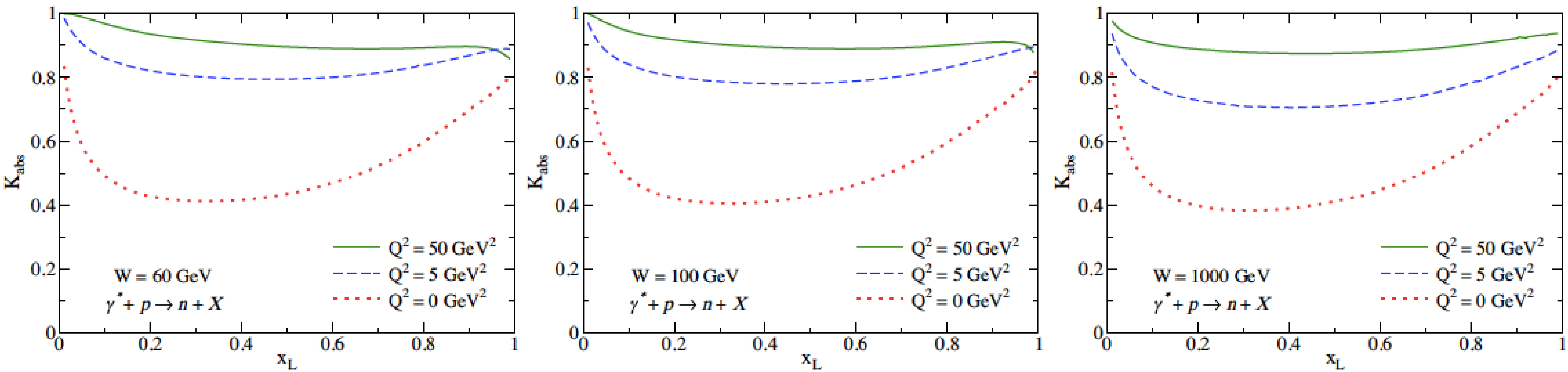

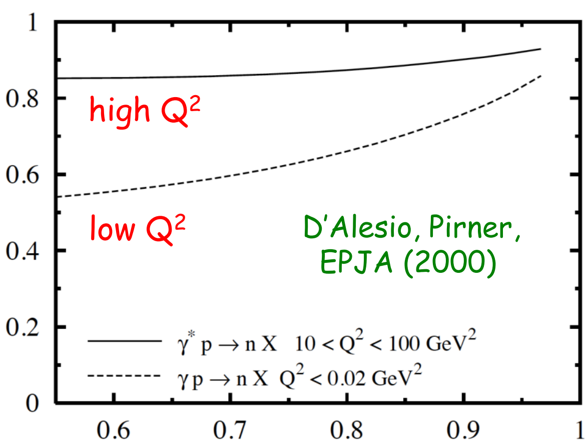

Weak energy dependence !

Stronger absorption !

Carvalho, Gonçalves, FSN, Spiering, PRD 103 (2016) 032021

Leading Lambda Production

Same formulas

Change masses and couplings

$$\sigma_{d\pi} \rightarrow \sigma_{dK}$$

$$\sigma_{dn} \rightarrow \sigma_{d\Lambda}$$

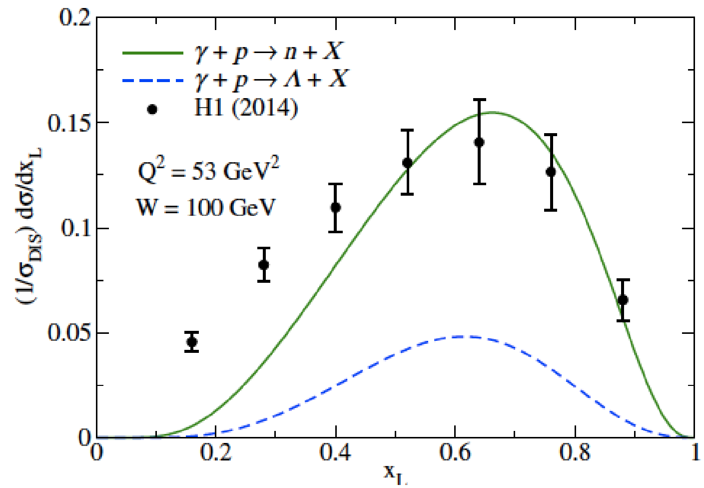

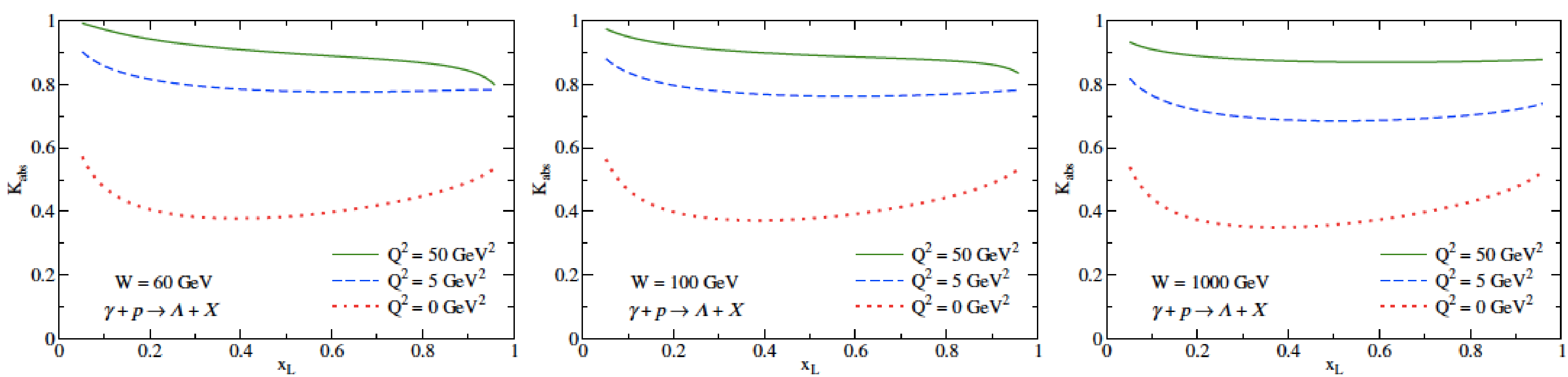

Comparing neutron and Lambda absorption

A dipole interacts more with a neutron or with a Lambda ?

$$\sigma_{d\Lambda} = \sigma_{dn}$$

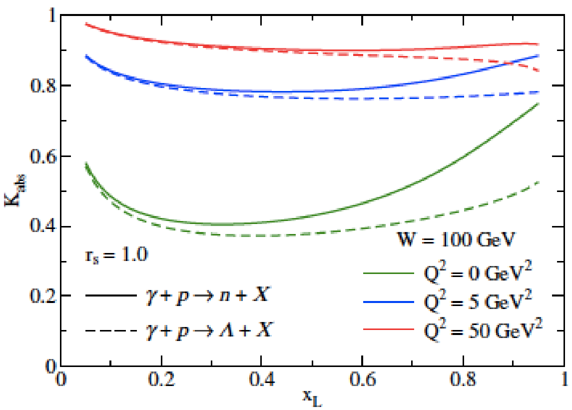

$$\sigma_{d\Lambda} = 0.8\,\sigma_{dn}$$

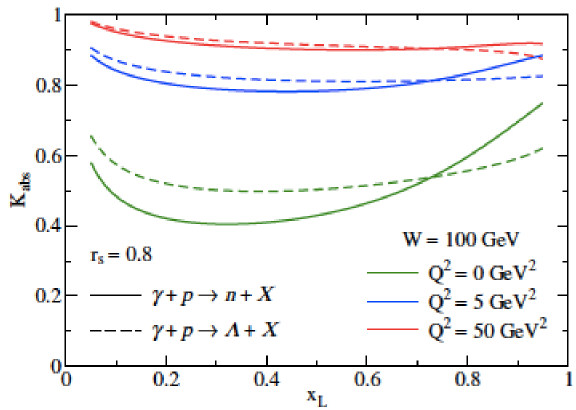

$$\sigma_{d\Lambda} = 0.5\,\sigma_{dn}$$

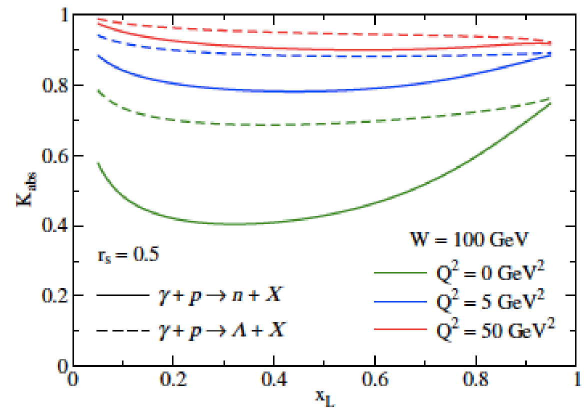

The relevant energy:

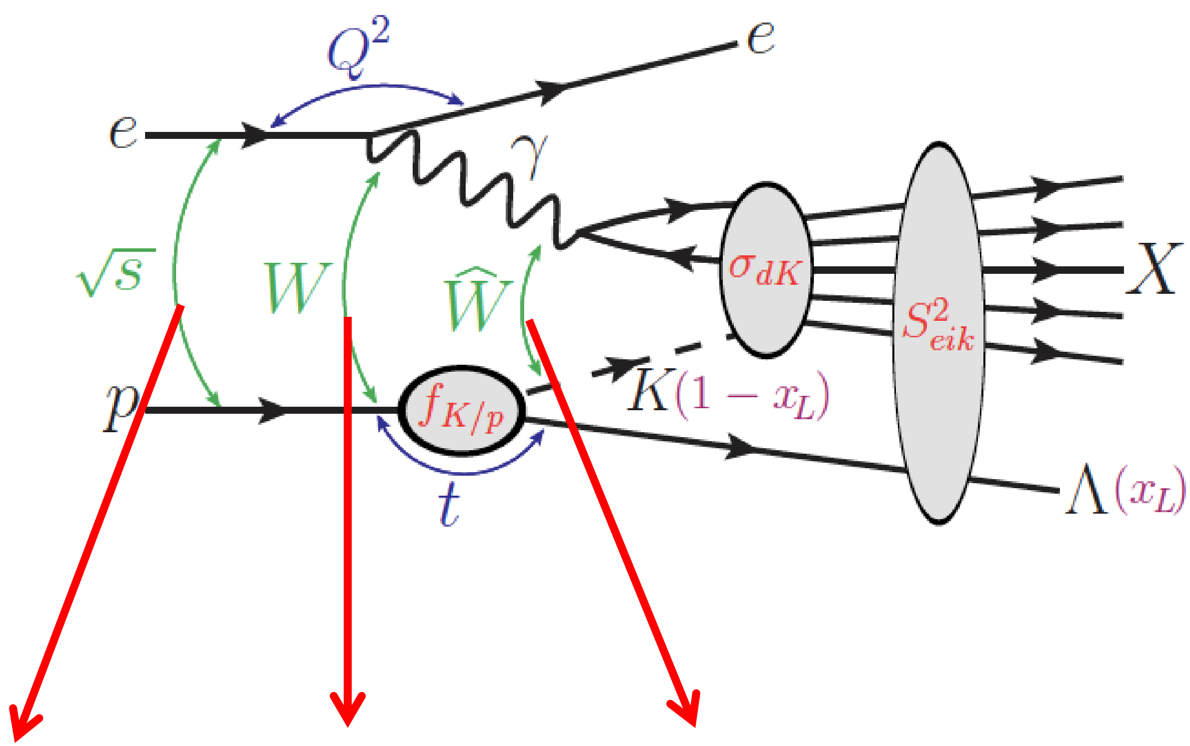

HERA 360 100-200 50 - 100 (GeV)

Guidance from data :

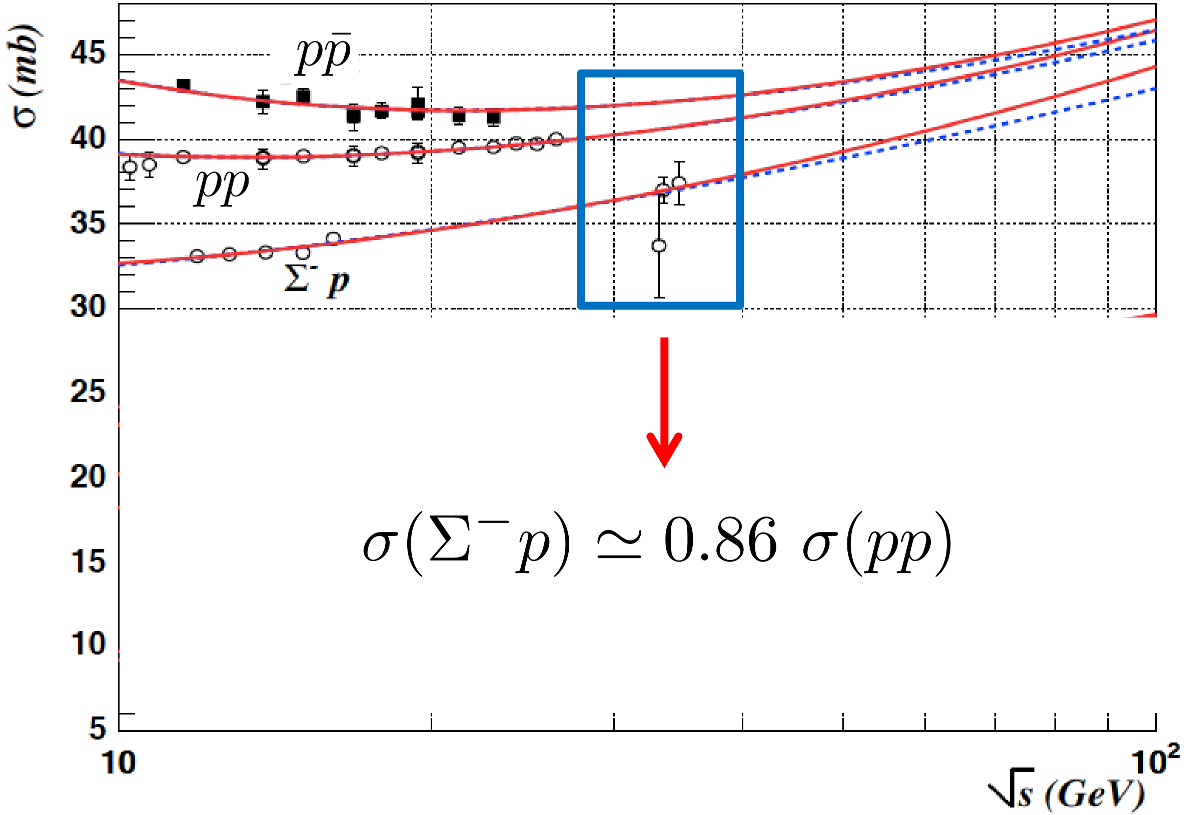

$$\sigma(\Sigma^- p) \simeq 0.86\ \sigma(pp)$$

Luna, Menon and Montanha, NPA 745 (2004) 104

The relevant energy:

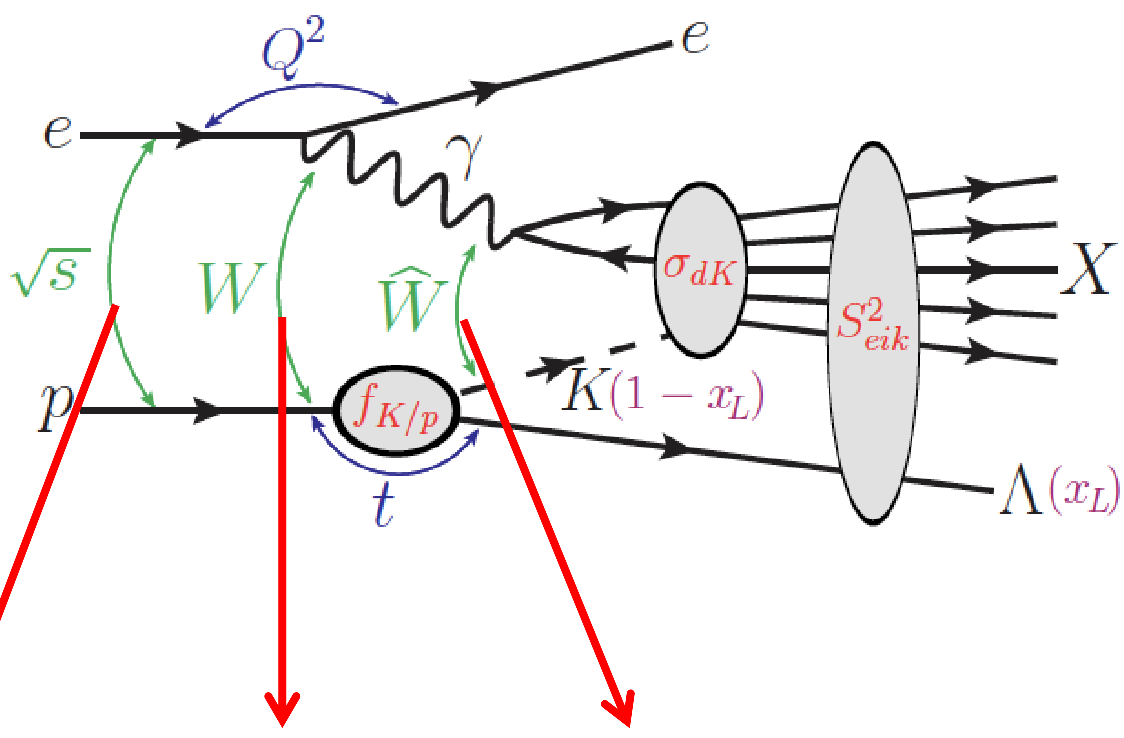

HERA	360	100-200	50 - 100	(GeV)
LeHC		~1000	~500	
JLab		~10-20	~5-10	

Connection to low energy hadron physics

Bounds on the dipole-Lambda cross section from meson-baryon reactions

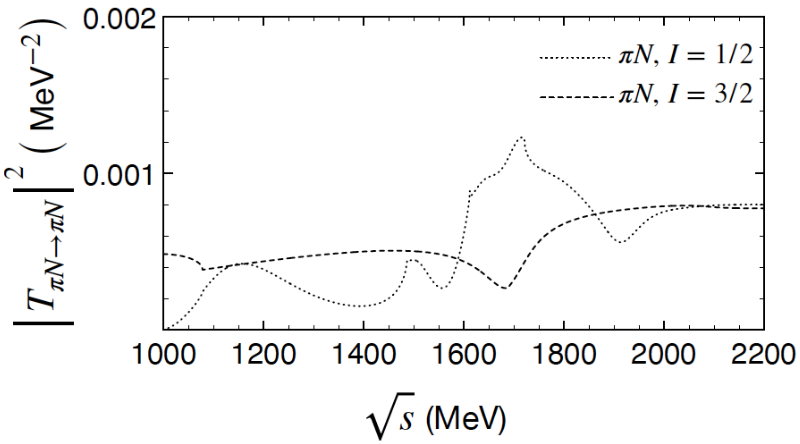

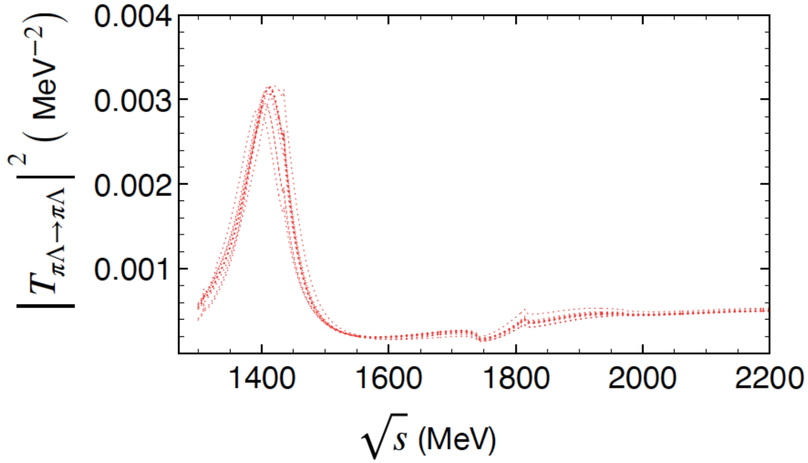

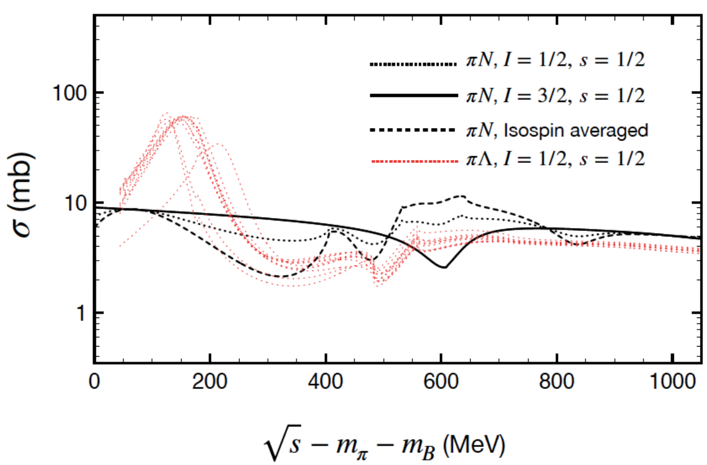

$$\sigma_{d\Lambda} = 0.8\,\sigma_{dn}$$

Work in progress...

Conclusion

We need the Sullivan process ("pion cloud") !

Leading neutron/Lambda production can be low x physics !

Leading Lambda production is feasible (large cross section)

We really need absorption !

Lambda are less absorbed than neutrons ?

Thank you !

Diffractive processes

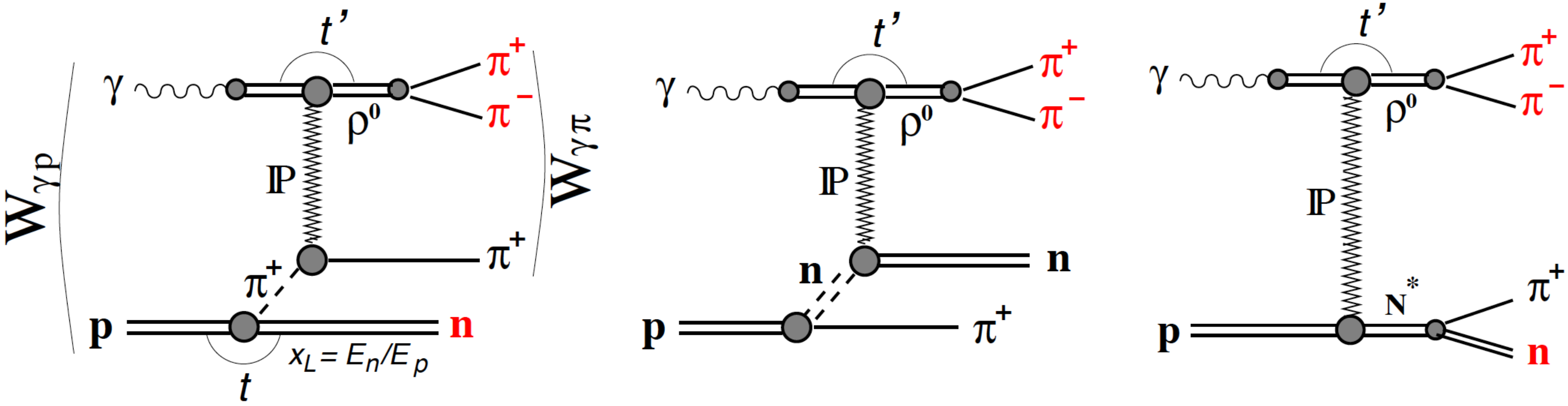

Summary

LN spectra in the dipole approach: several processes in the same framework

Not included:
- fragmentation
- $\Delta^+ \rightarrow \pi^+ n$
- ρ exchange

(small contribution or only at low x_L)

Uncertainties:
- "aditive quark model" $\frac{1}{3} < R_q < \frac{2}{3}$
- absorption $0.5 < K < 1$
- pion flux
- dipole cross section
- vector meson wave function

Exclusive production data: absorption is large

Extension to pp and pA

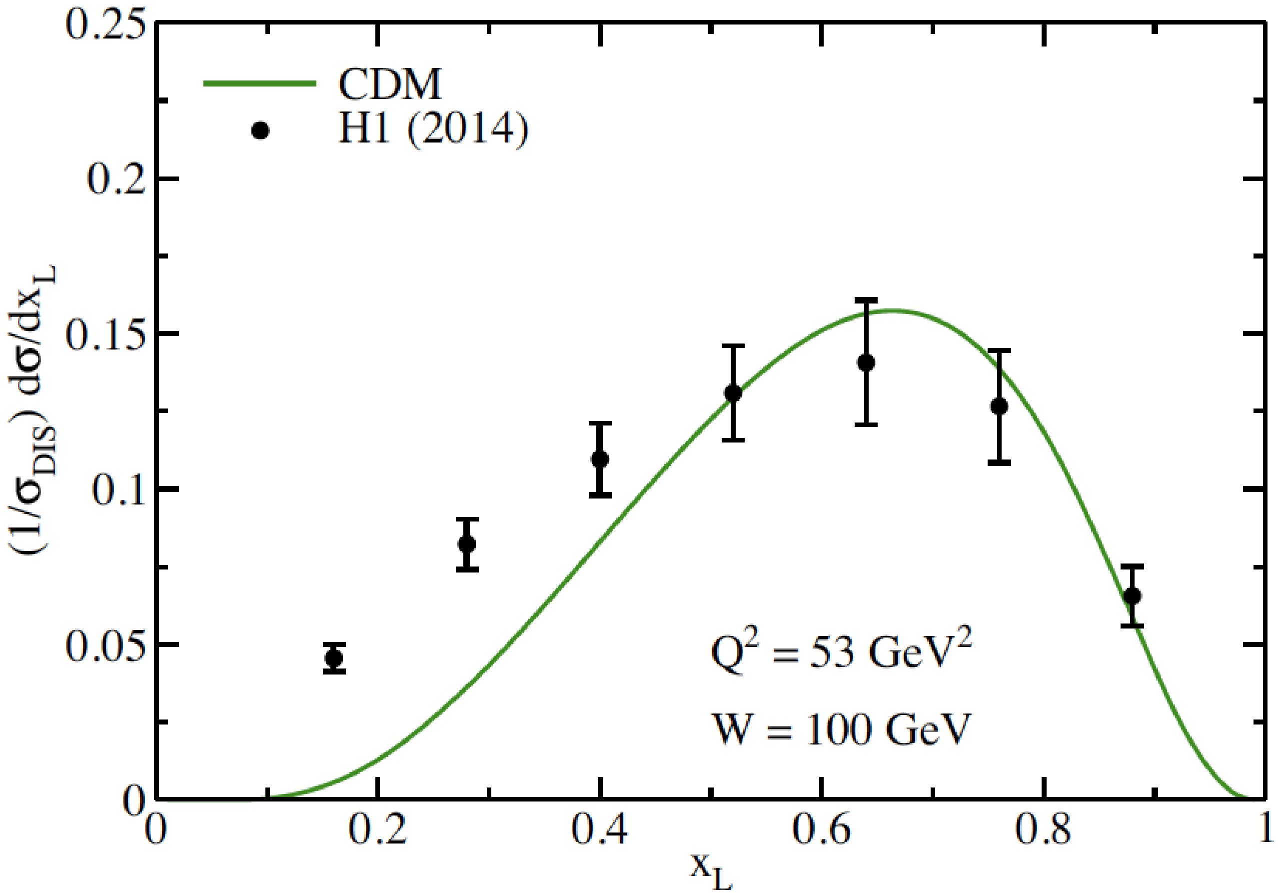

CDM
H1 (2014)
$Q^2 = 53$ GeV^2
W = 100 GeV
$(1/\sigma_{DIS})\, d\sigma/dx_L$
x_L
0
0.05
0.1
0.15
0.2
0.25
0.2
0.4
0.6
0.8
1

At JLAB energies :

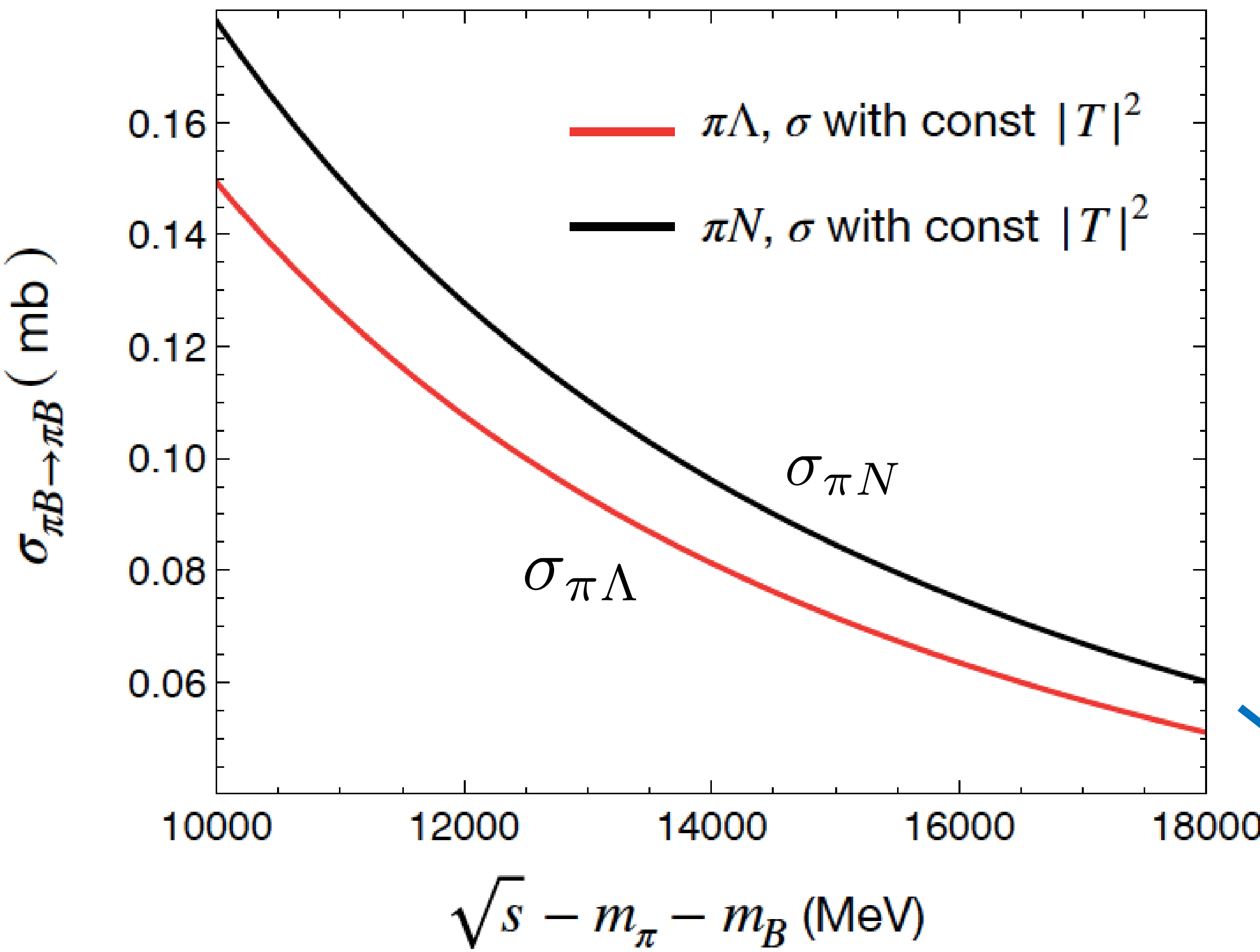

$$\sigma_{d\Lambda} = 0.8\,\sigma_{dn}$$

Work in progress...

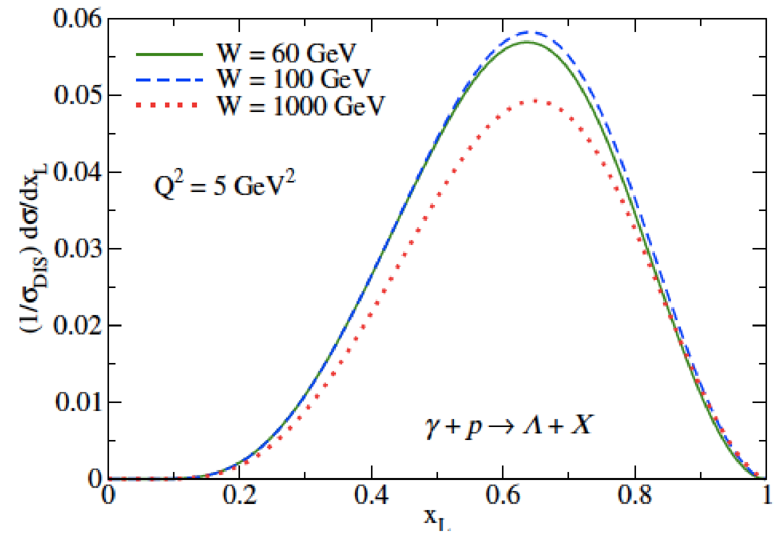

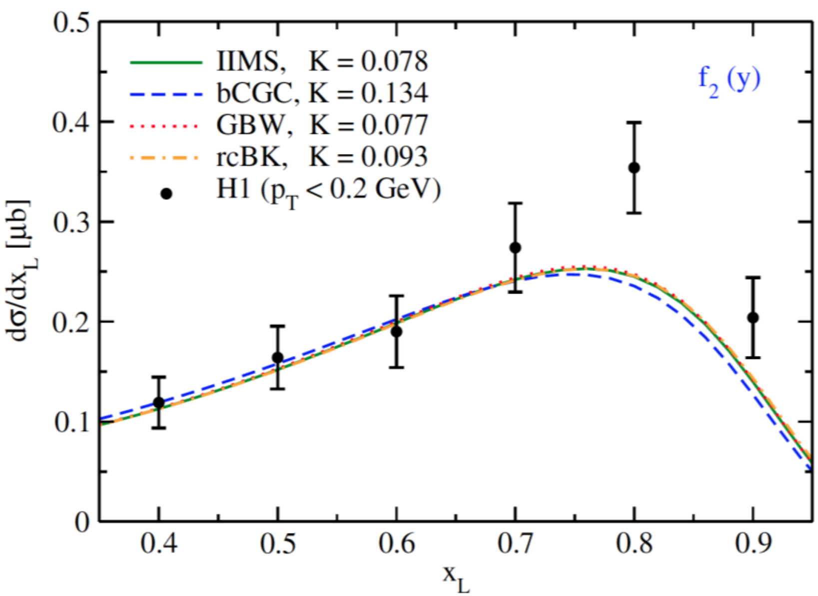

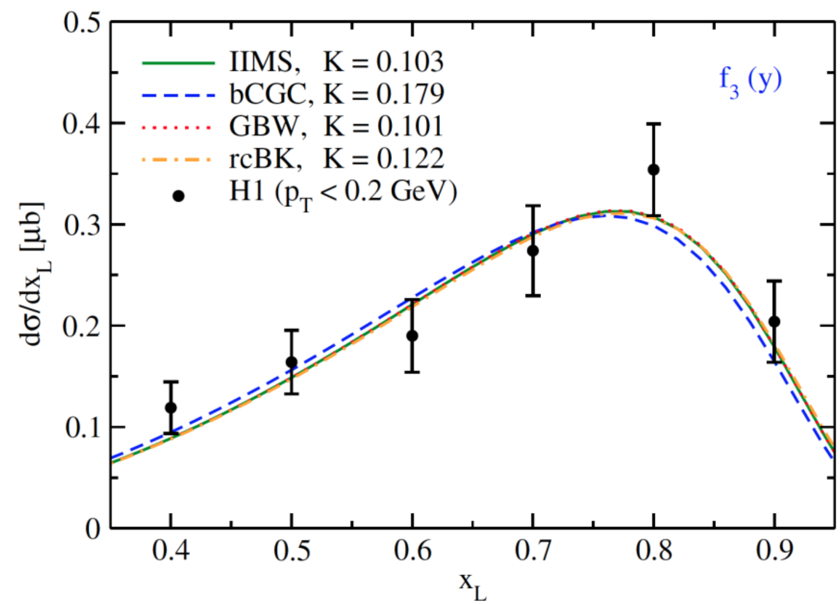

Gonçalves, FSN, Spiering, PRD 93 (2016) 054025

* $\frac{1}{3} < R_q < \frac{2}{3}$ $\quad 0.5 < K < 1$

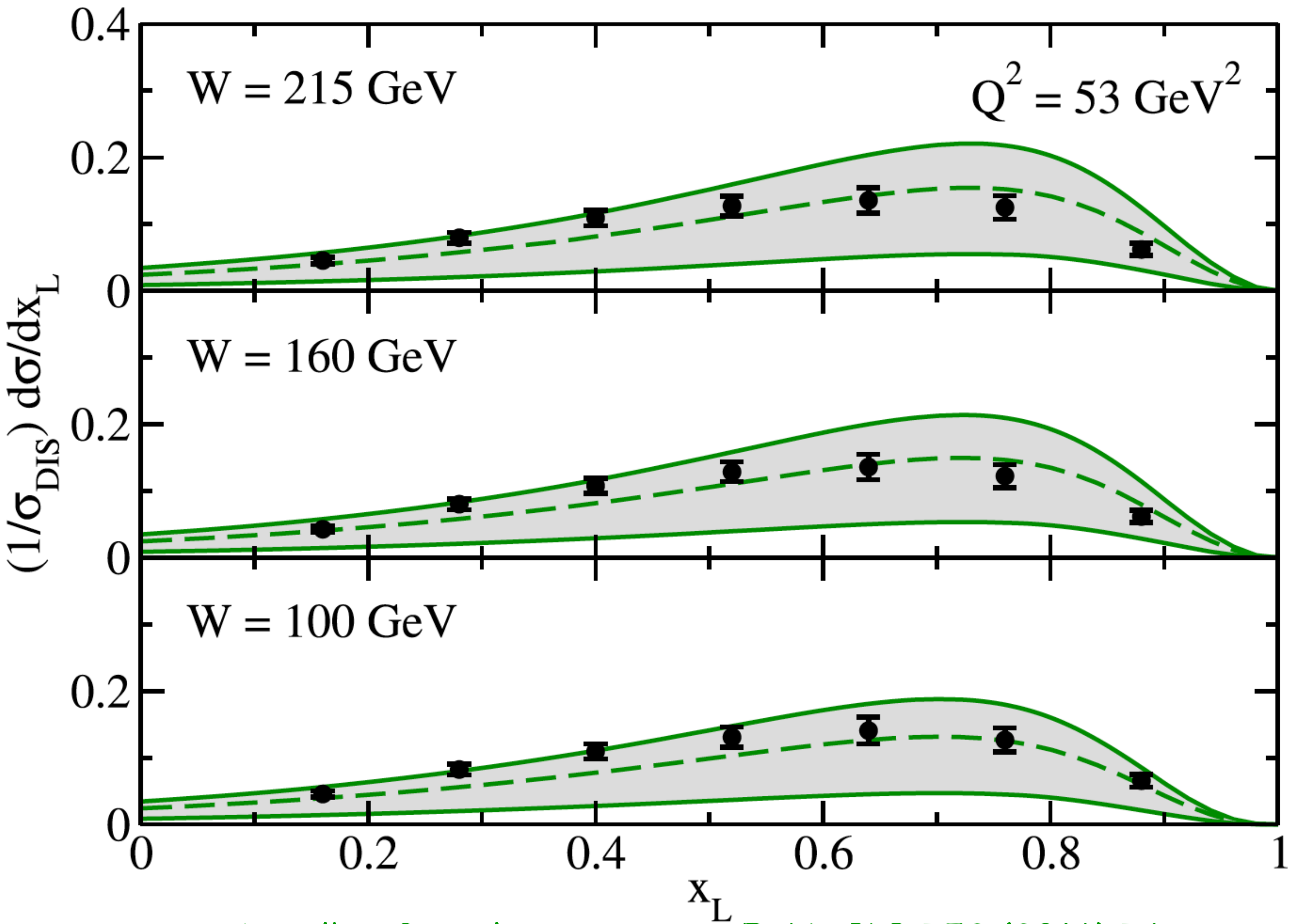

Carvalho, Gonçalves, Spiering, FSN, PLB 752 (2016) 76

* S. Chekanov *et al*. [ZEUS Collaboration], Nucl. Phys. **B637** 3 (2002) 3

Predictions

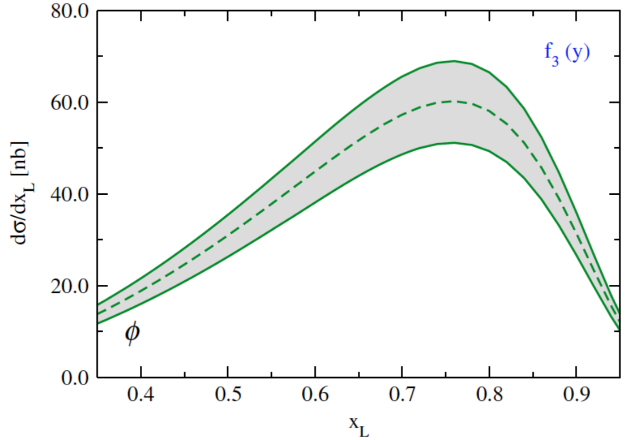

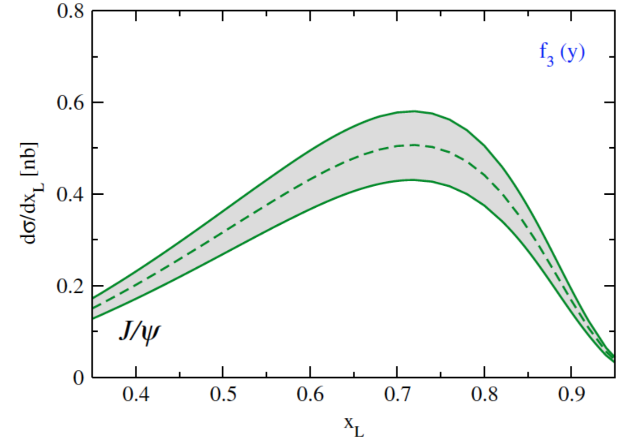

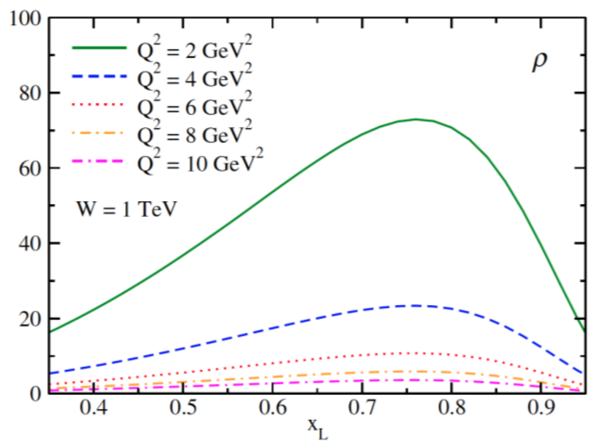

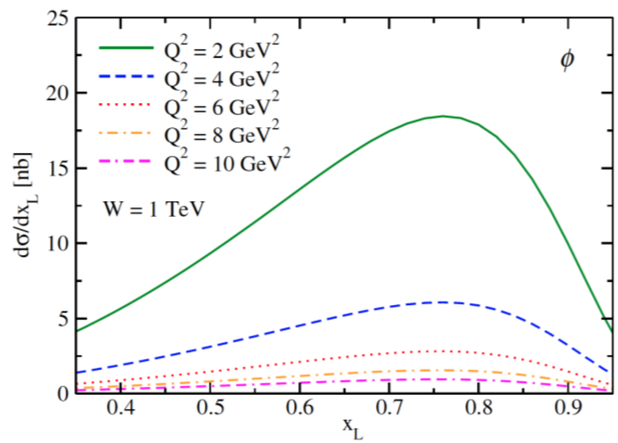

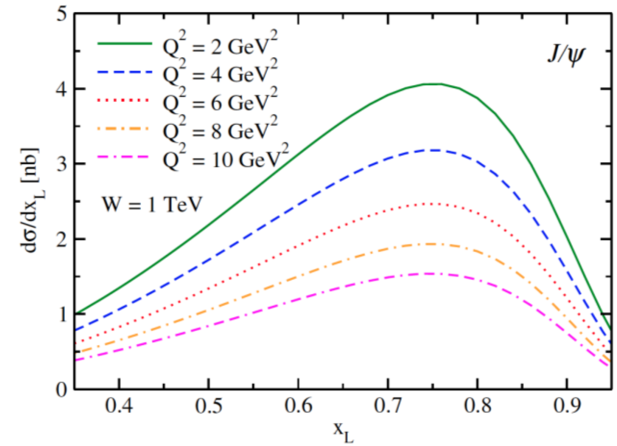

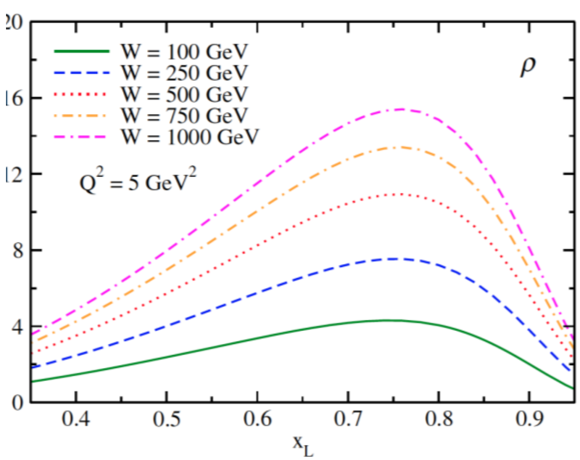

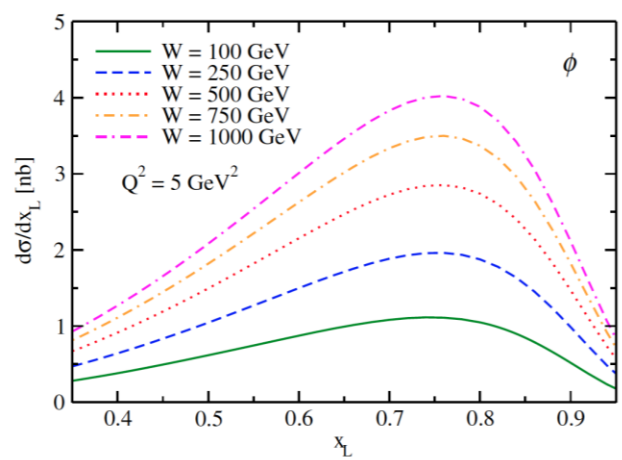

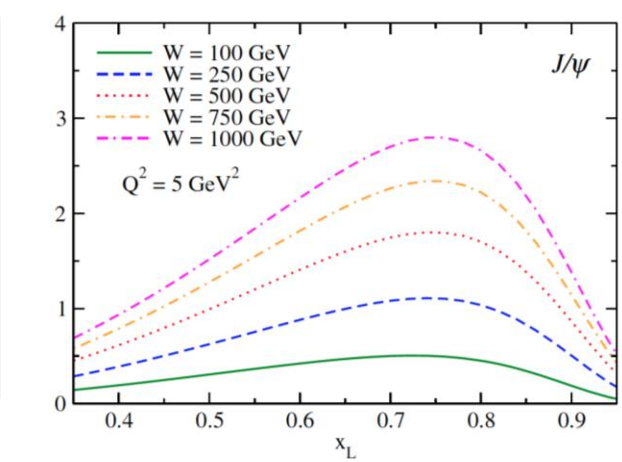

Predictions

p - p **p - A**

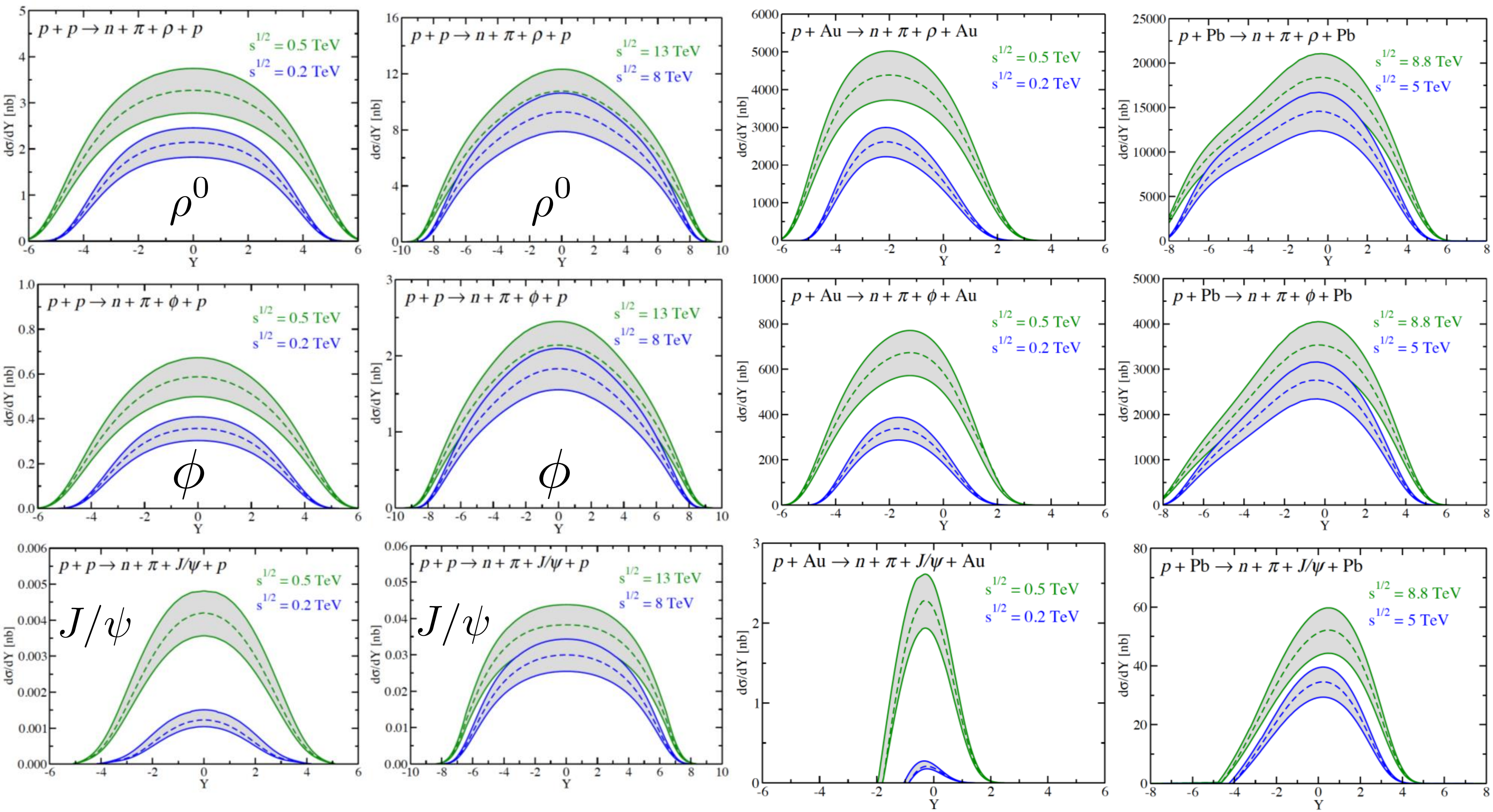

Gonçalves, Moreira, FSN, Spiering, PRD 94 (2016) 014009

Predictions

p - p

$\sigma(V)$ [nb]		$\sqrt{s} = 0.2$ TeV	$\sqrt{s} = 0.5$ TeV	$\sqrt{s} = 8.0$ TeV	$\sqrt{s} = 13.0$ TeV
ρ	K_{min}	12.17	22.06	90.12	110.51
	K_{med}	14.34	25.98	106.12	130.14
	K_{max}	16.42	29.75	121.54	149.04
ϕ	K_{min}	1.83	3.58	16.67	20.73
	K_{med}	2.15	4.21	19.63	24.42
	K_{max}	2.46	4.83	22.48	27.96
J/ψ	K_{min}	0.0042	0.019	0.25	0.35
	K_{med}	0.0049	0.022	0.30	0.42
	K_{max}	0.0064	0.026	0.34	0.48

p - A

$\sigma(V)$ [nb]		$\sqrt{s} = 0.2$ TeV	$\sqrt{s} = 0.5$ TeV	$\sqrt{s} = 5.0$ TeV	$\sqrt{s} = 8.8$ TeV
ρ	K_{min}	9176.88	20819.90	102785.00	139110.00
	K_{med}	10807.00	24518.30	121043.00	163821.00
	K_{max}	12376.70	28079.50	138625.00	187616.00
ϕ	K_{min}	1090.55	2863.67	17326.20	24154.90
	K_{med}	1278.41	3386.65	20403.80	28445.60
	K_{max}	1470.81	3862.20	23367.50	32577.30
J/ψ	K_{min}	0.19	3.94	135.53	234.50
	K_{med}	0.23	4.65	159.61	276.16
	K_{max}	0.32	5.65	184.04	317.05

Back ups

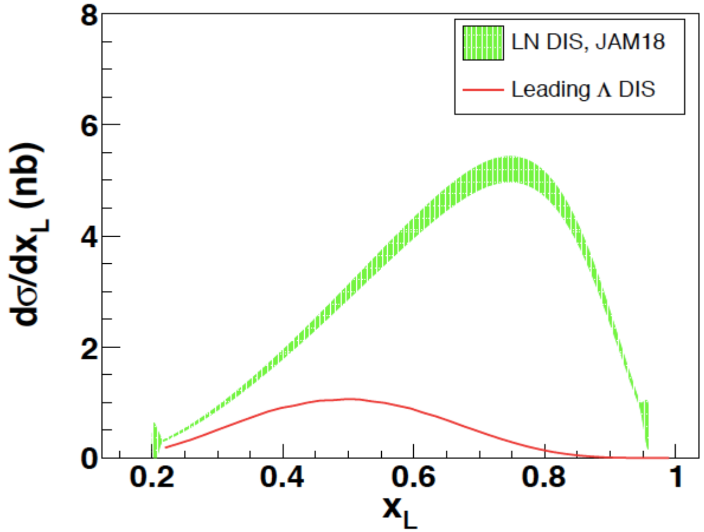

Xie,Wang,Han,Chen, arXiv:2109.08483

$$e^- + p \to e^- + X + n$$

V. Andreev et al., EJPC 74, 2915 (2014)

$$e^- + p \to e^- + \rho^0 + \pi^+ + n$$

V. Andreev et al., EJPC 76, 41 (2016)

Chiral perturbation theory

$$f_{\pi/p}(y, k_T^2) = \frac{g_A^2 m_p^2}{4\pi f_\pi^2} \int_0^{p_{T\,max}^2} dk_t^2 \frac{y(k_t^2 + y^2 m_p^2)}{[k_T^2 + y m_p^2 + (1-y) m_\pi^2]^2}$$

Salamu, Ji, Melnitchouk, Wang, PRL (2015)
Burkardt et al., PRD (2013)

$$\mathcal{L}_{\pi N}^{\mathrm{PS}} = -g_{\pi NN} \bar{\psi}_N i \gamma_5 \boldsymbol{\tau} \cdot \boldsymbol{\pi} \psi_N, \longrightarrow \mathcal{L}_{\pi N} = \frac{g_A}{2f_\pi} \bar{\psi}_N \gamma^\mu \gamma_5 \boldsymbol{\tau} \cdot \partial_\mu \boldsymbol{\pi} \psi_N - \frac{1}{(2f_\pi)^2} \bar{\psi}_N \gamma^\mu \boldsymbol{\tau} \cdot (\boldsymbol{\pi} \times \partial_\mu \boldsymbol{\pi}) \psi_N,$$

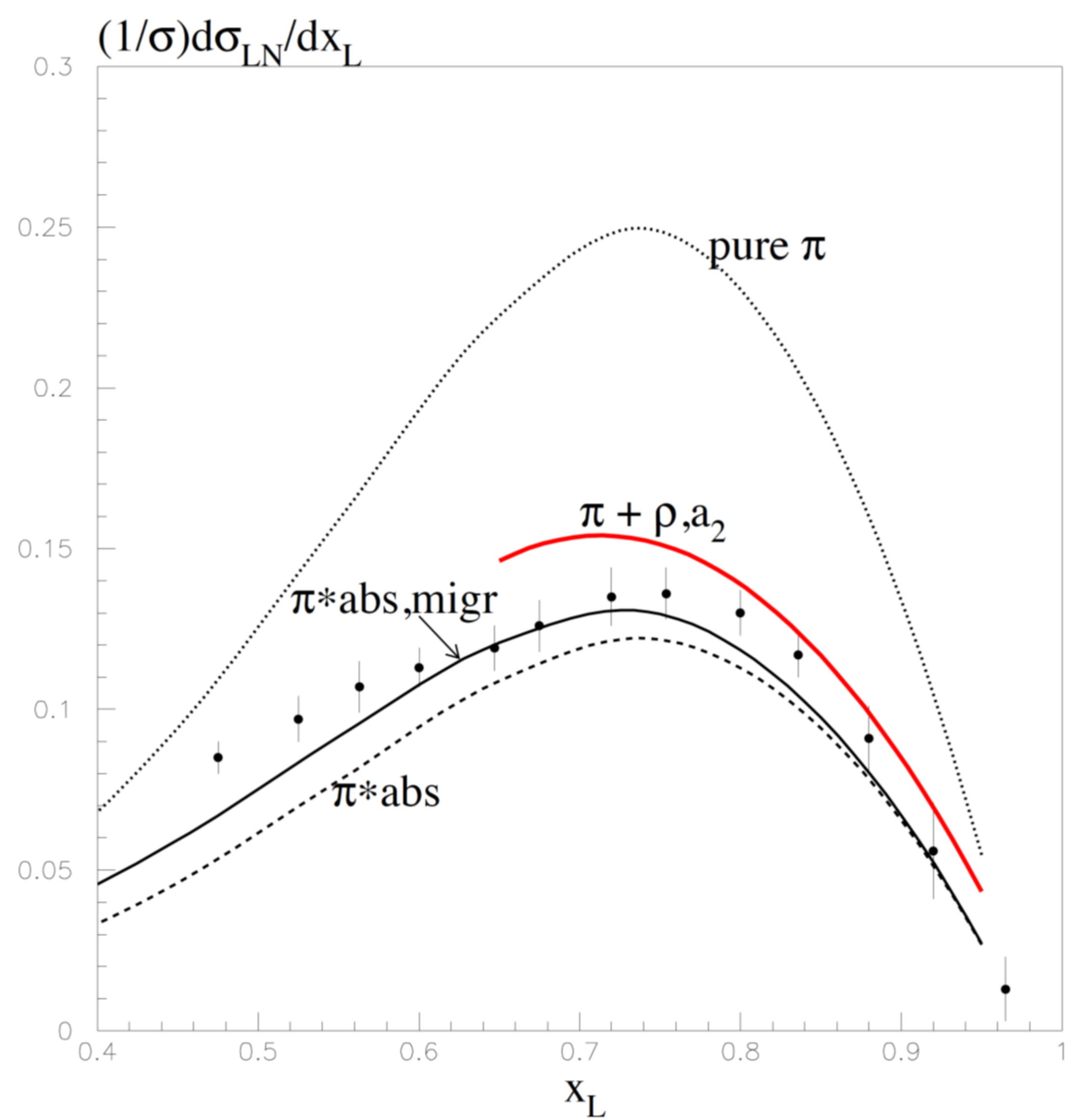

Khose, Martin, Ryskin, hep-ph/0606213

ρ^0 with Forward Neutron

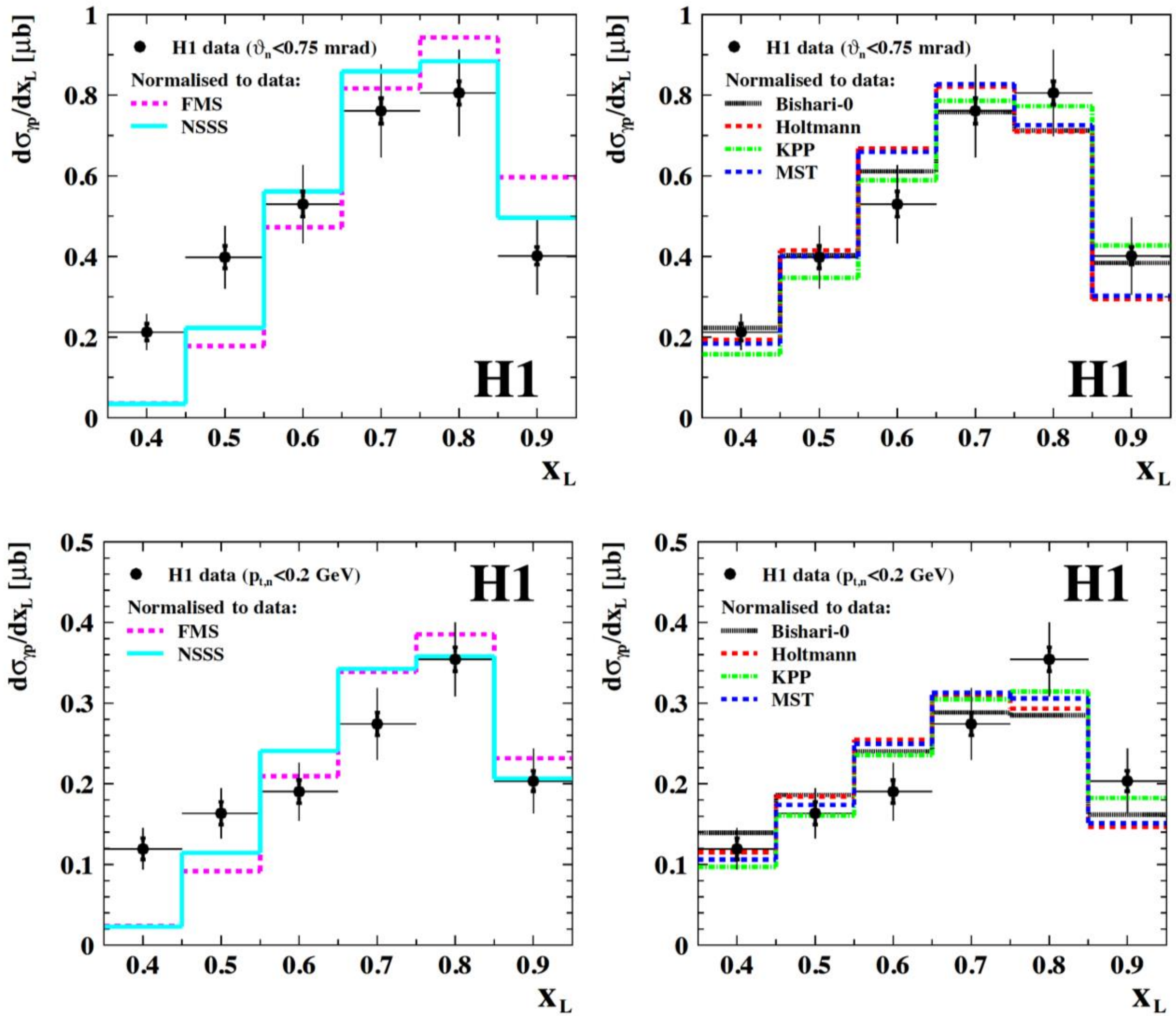

H1: V. Andreev et al., EJPC 76, 41 (2016)

Energy dependence and Feynman scaling

Kaidalov, Khose, Martin, Ryskin, hep-ph/0602215

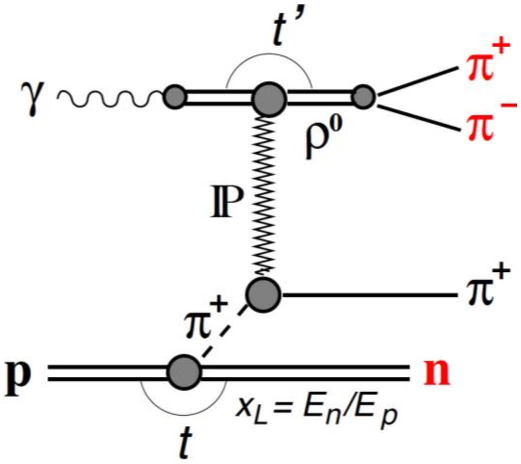

$$\frac{d^2\sigma(W,Q^2,x_L,t)}{dx_L dt} = f_{\pi/p}(x_L,t)\underline{\sigma_{\gamma^*\pi}(\hat{W}^2,Q^2)}$$

$$\underline{\sigma_{\gamma^*\pi}(\hat{x},Q^2)} = \frac{2}{3}\sigma_{\gamma^*p}(\hat{x},Q^2) = \frac{2}{3}\int_0^1 dz \int d^2r \sum_{L,T} |\Psi_{T,L}(z,r,Q^2)|^2 \underline{\sigma_{dip}(\hat{x},r)}$$

$$\underline{\sigma_{dip}(r,\hat{x})} = 2\int d^2\boldsymbol{b}\,\mathcal{N}(r,\hat{x},\boldsymbol{b}) = \sigma_0\ [1 - exp(-\frac{(Q_s(\hat{x})r)^2}{4})]$$

$$Q_s^2(\hat{x}) = Q_0^2\left(\frac{x_0}{\hat{x}}\right)^\lambda$$

$$Q_s^2 \to 0 \quad (\text{low} \quad W)$$

$$\sigma_{dip}(r,\hat{x}) \simeq \sigma_0\,\frac{Q_s^2(\hat{x})r^2}{4} \simeq \sigma_0\,Q_0^2\,x_0{}^\lambda[\frac{(1-x_L)W^2+Q^2}{Q^2+m_f^2}]^\lambda$$

linear

$$Q_s^2 \to \text{large} \quad (\text{high} \quad W)$$

$$\sigma_{dip}(r,\hat{x}) = \sigma_0\,\mathcal{N}(r,\hat{x}) \simeq \sigma_0$$

saturation

Future:

TeV electron-proton collider

Paul Newman's talk

Claire Gwenlan's talk

Very High Energy electron-proton collider (VHEeP)

Caldwell, Wing arXiv:1509.00235

Learn more about the pion structure function

Leading neutrons in Deep Inelastic Scattering

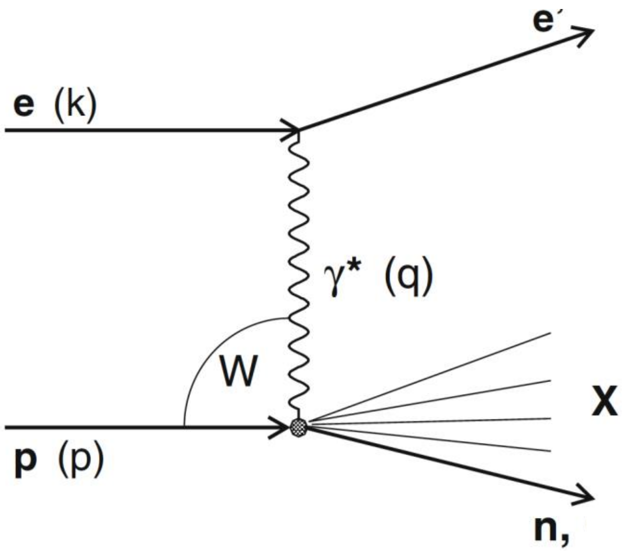

normal DIS
with quark fragmentation

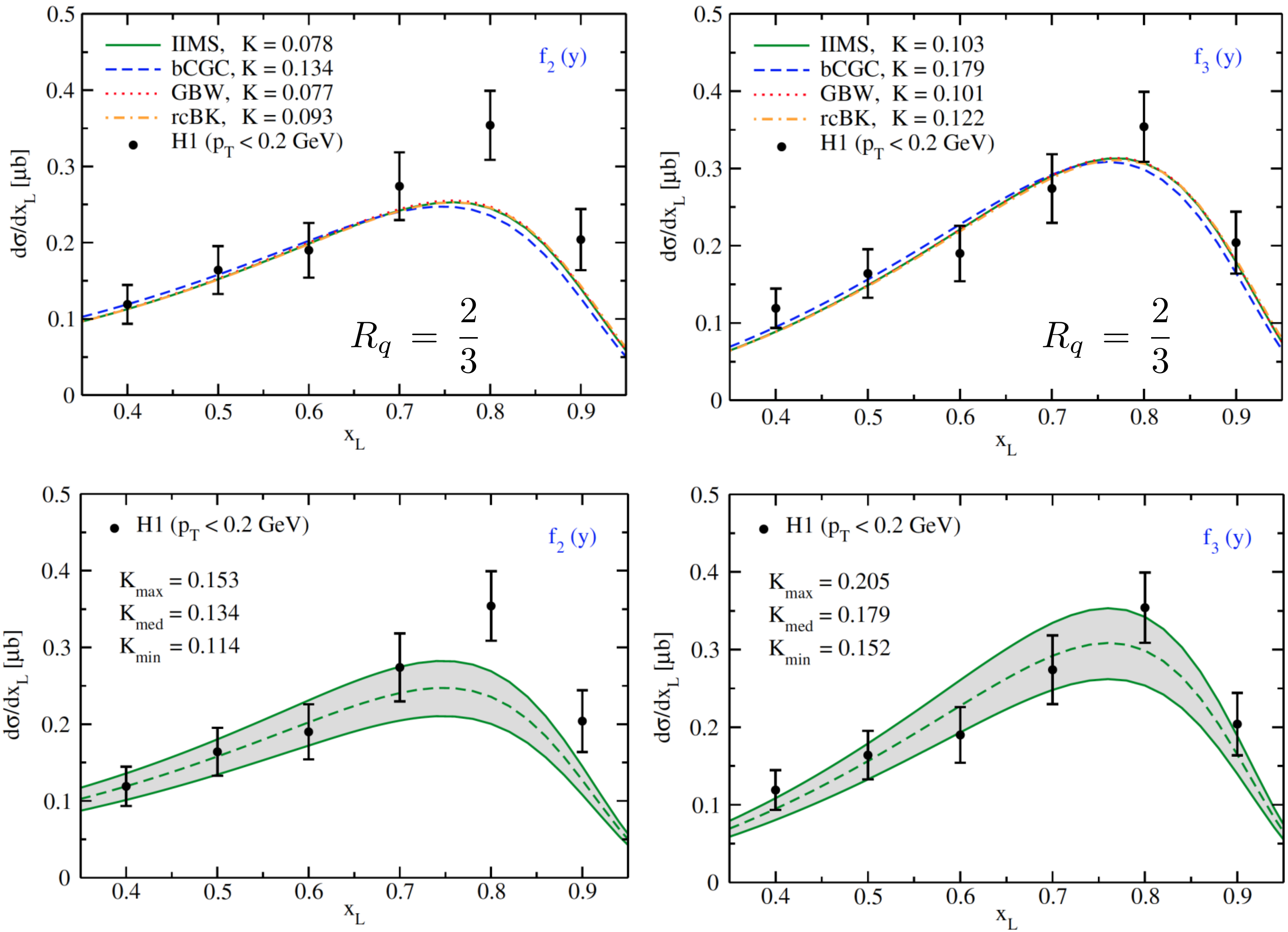

Gonçalves, FSN, Spiering, PRD 93 (2016) 054025

$$\frac{d^2\sigma(W, Q^2, x_L, t)}{dx_L dt} = f_{\pi/p}(x_L, t)\underline{\sigma_{\gamma^*\pi}(\hat{W}^2, Q^2)}$$

$$\frac{d^2\sigma(W,Q^2,x_L,t)}{dx_L\,dt} = f_{\pi/p}(x_L,t)\sigma_{\gamma^*\pi}(\hat{W}^2,Q^2)$$

$$\sigma_{\gamma^*\pi}(\hat{x},Q^2) = \frac{2}{3}\sigma_{\gamma^*p}(\hat{x},Q^2) = \frac{2}{3}\int_0^1 dz \int d^2r \sum_{L,T} |\Psi_{T,L}(z,r,Q^2)|^2 \sigma_{dip}(\hat{x},r)$$

$$\frac{d^2\sigma(W,Q^2,x_L,t)}{dx_L\,dt} = f_{\pi/p}(x_L,t)\sigma_{\gamma^*\pi}(\hat{W}^2,Q^2)$$

$$\sigma_{\gamma^*\pi}(\hat{x},Q^2) = \frac{2}{3}\sigma_{\gamma^*p}(\hat{x},Q^2) = \frac{2}{3}\int_0^1 dz \int d^2r \sum_{L,T} |\Psi_{T,L}(z,r,Q^2)|^2 \sigma_{dip}(\hat{x},r)$$

$$\sigma_{dip}(r,\hat{x}) = 2\int d^2\boldsymbol{b}\,\mathcal{N}(r,\hat{x},\boldsymbol{b}) = \sigma_0\ [1 - exp(-\frac{(Q_s(\hat{x})r)^2}{4})]$$

$$Q_s^2(\hat{x}) = Q_0^2\left(\frac{x_0}{\hat{x}}\right)^{\lambda}$$

$$\hat{x} = \frac{Q^2 + m_f^2}{\hat{W}^2 + Q^2} = \frac{Q^2 + m_f^2}{(1 - x_L)W^2 + Q^2}$$

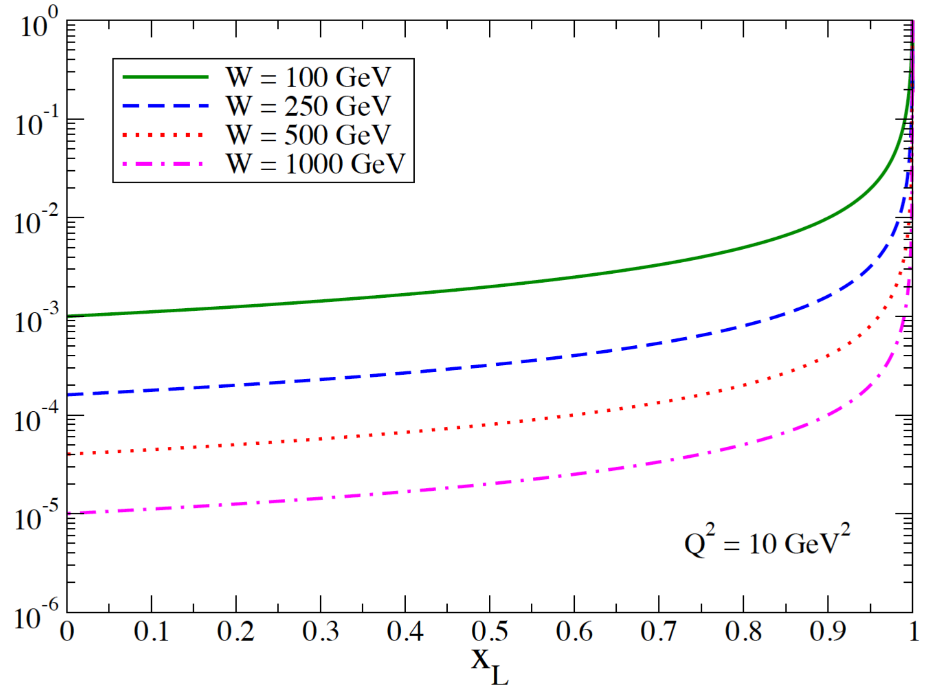

Leading neutron production
can be low x physics !

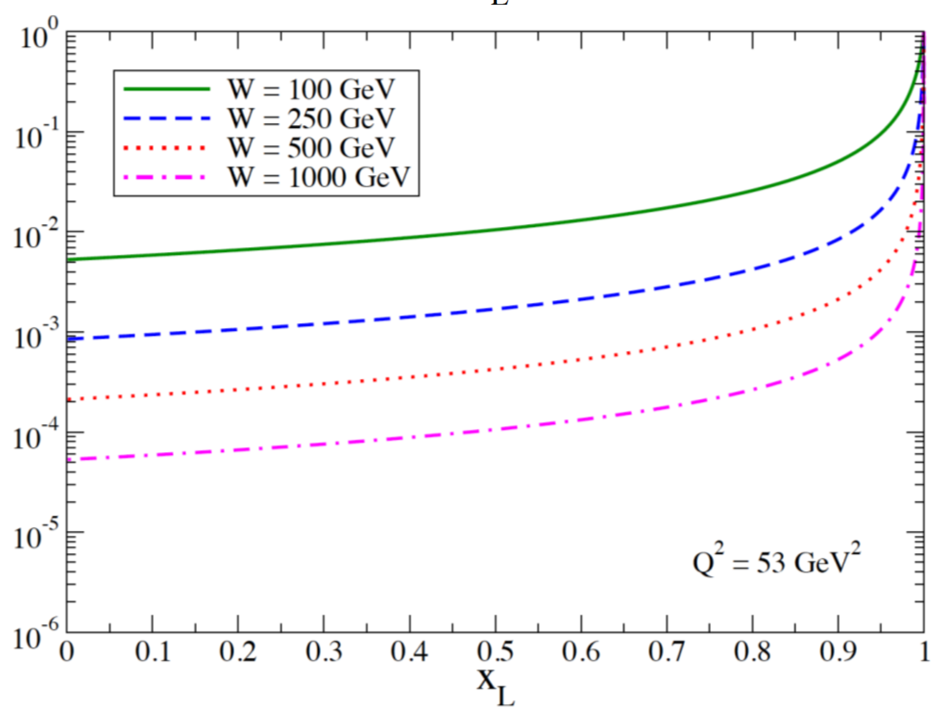

Linear:

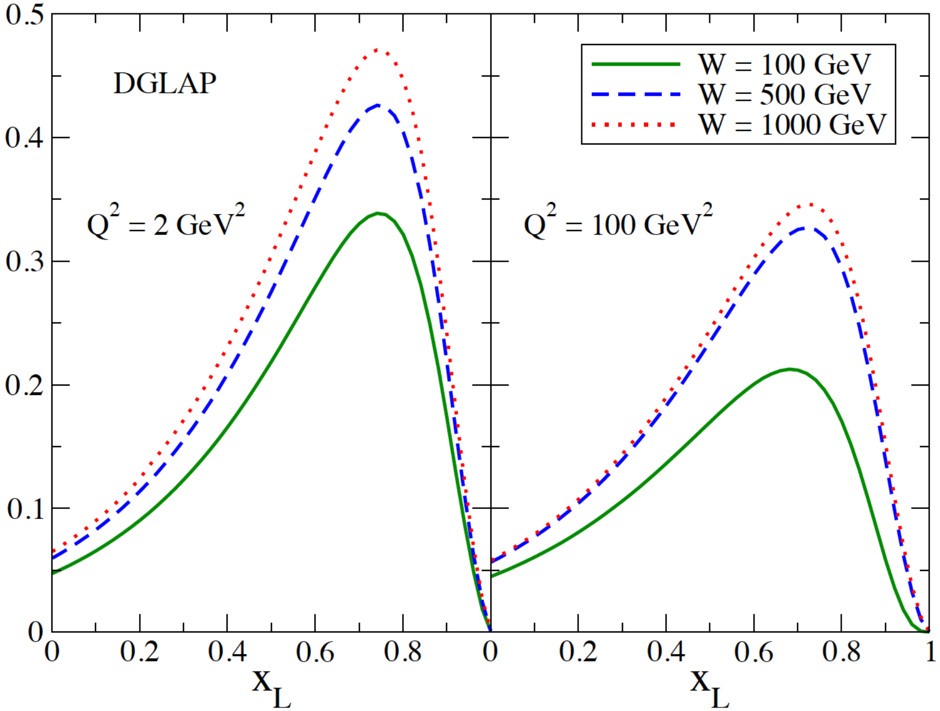

Saturation:

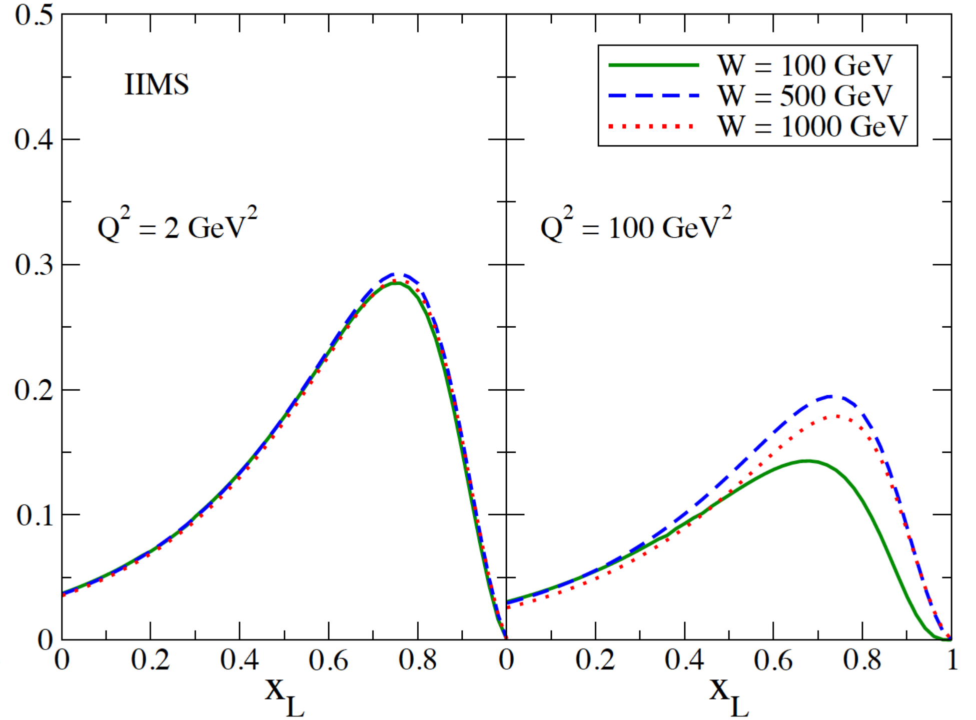

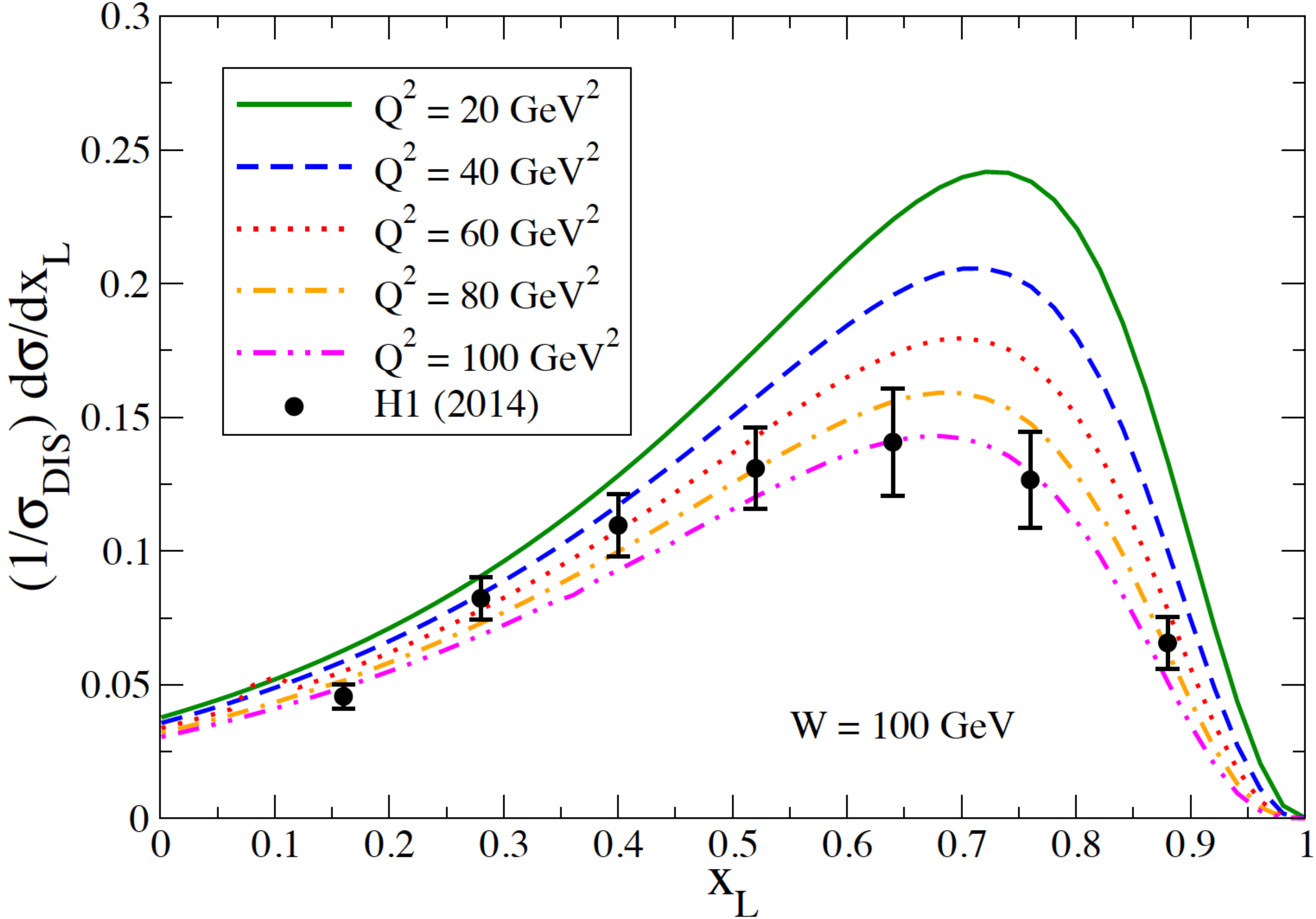

$Q^2 = 20\ GeV^2$
$Q^2 = 40\ GeV^2$
$Q^2 = 60\ GeV^2$
$Q^2 = 80\ GeV^2$
$Q^2 = 100\ GeV^2$
H1 (2014)
W = 100 GeV
$(1/\sigma_{DIS})\ d\sigma/dx_L$
x_L
0
0.05
0.1
0.15
0.2
0.25
0.3
0
0.1
0.2
0.3
0.4
0.5
0.6
0.7
0.8
0.9
1

Energy dependence and Feynman scaling

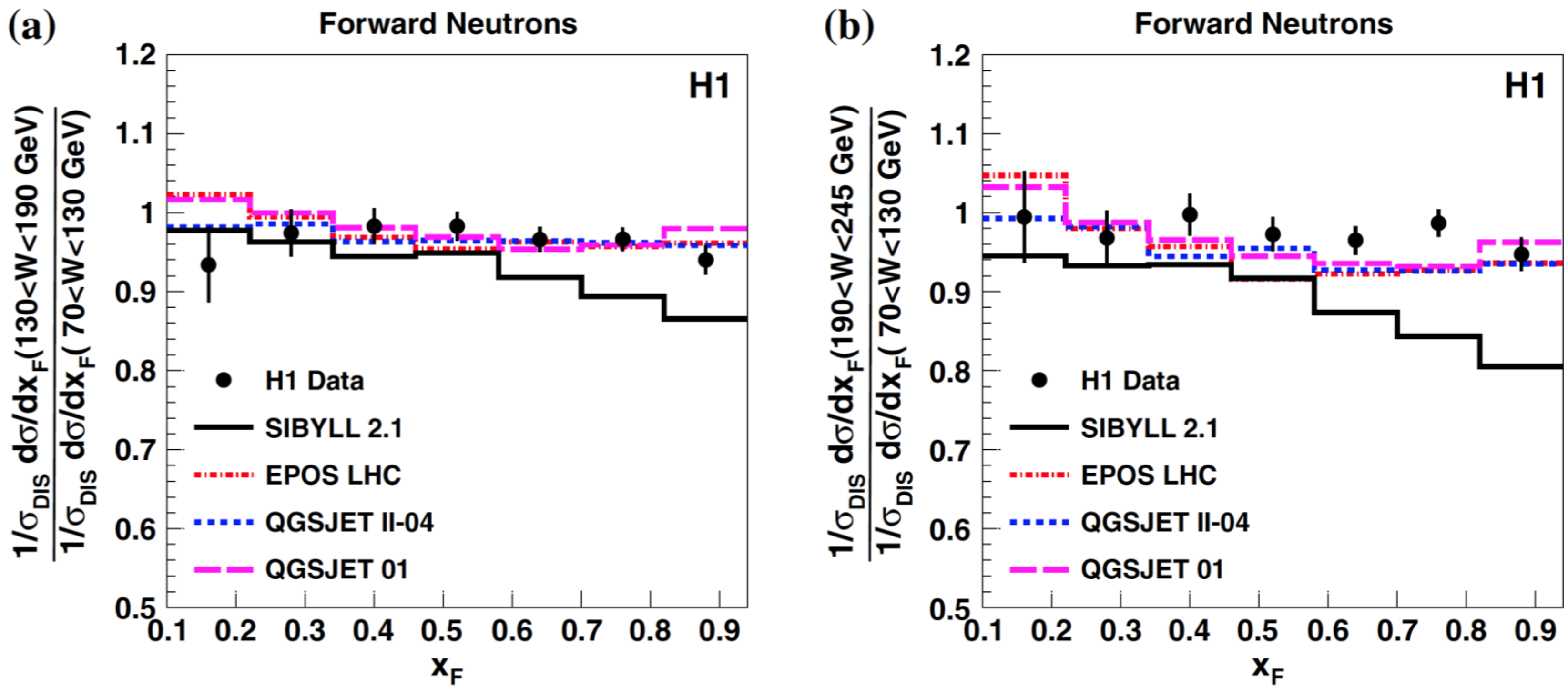

W ranges for cross sections $\frac{1}{\sigma_{DIS}}\frac{d\sigma}{dx_F}$

$$70 < W < 130\ \text{GeV}$$

$$130 < W < 190\ \text{GeV}$$

$$190 < W < 245\ \text{GeV}$$

Data from H1 and ZEUS

NC DIS Selection	
$6 < Q^2 < 100\ \mathrm{GeV}^2$	
$0.05 < y < 0.6$	
$70 < W < 245\ \mathrm{GeV}$	
Forward photons	**Forward neutrons**
$\eta > 7.9$	$\eta > 7.9$
$0.1 < x_F < 0.7$	$0.1 < x_F < 0.94$
$0 < p_T^* < 0.4\ \mathrm{GeV}$	$0 < p_T^* < 0.6\ \mathrm{GeV}$
W ranges for cross sections $\frac{1}{\sigma_{DIS}}\frac{\mathrm{d}\sigma}{\mathrm{d}x_F}$	
$70 < W < 130\ \mathrm{GeV}$	
$130 < W < 190\ \mathrm{GeV}$	
$190 < W < 245\ \mathrm{GeV}$	

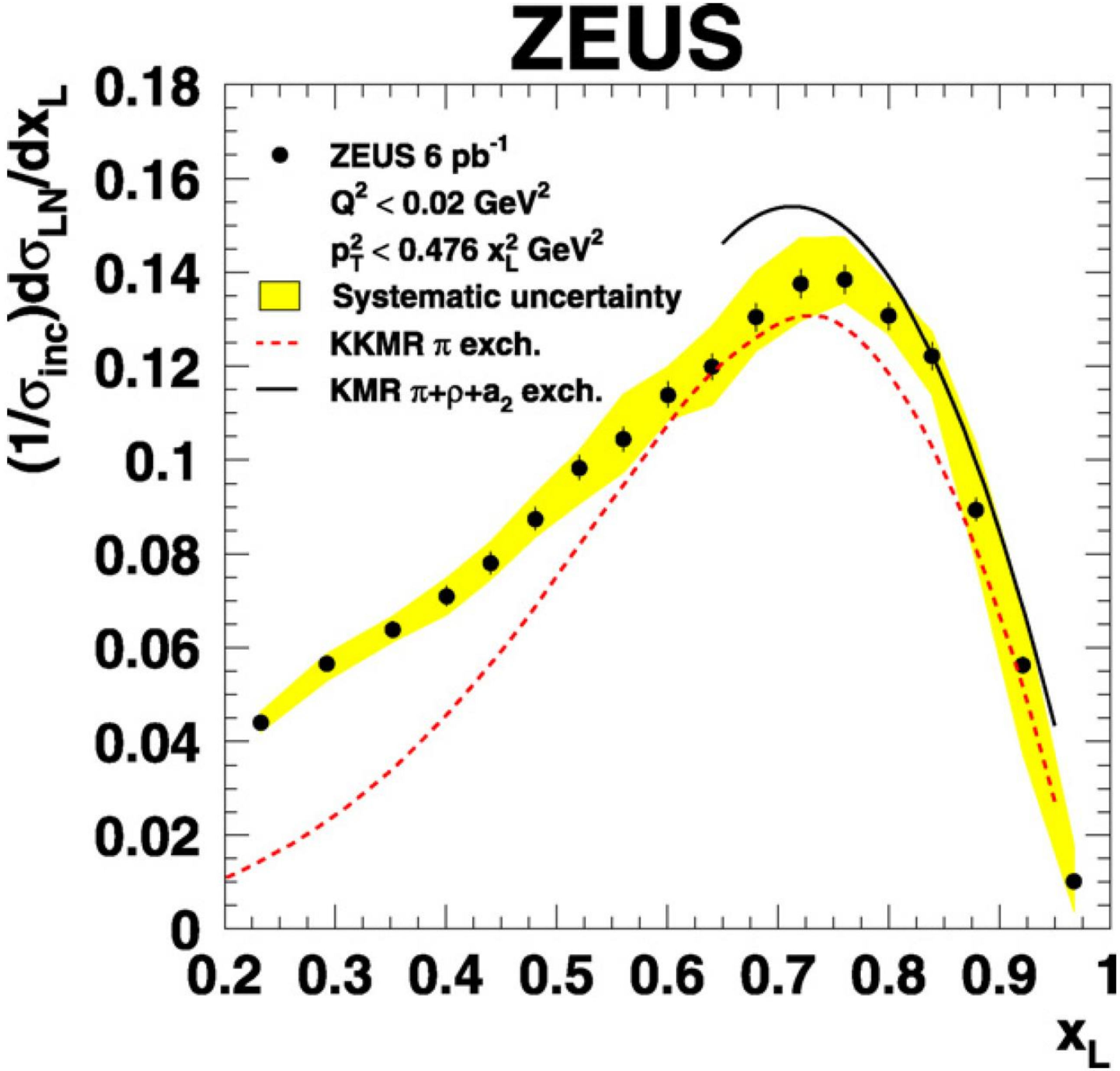

ZEUS
$(1/\sigma_{inc})d\sigma_{LN}/dx_L$
ZEUS 6 pb^{-1}
$Q^2 < 0.02$ GeV^2
$p_T^2 < 0.476\ x_L^2$ GeV^2
Systematic uncertainty
KKMR π exch.
KMR $\pi+\rho+a_2$ exch.
0
0.02
0.04
0.06
0.08
0.1
0.12
0.14
0.16
0.18
0.2
0.3
0.4
0.5
0.6
0.7
0.8
0.9
1
x_L

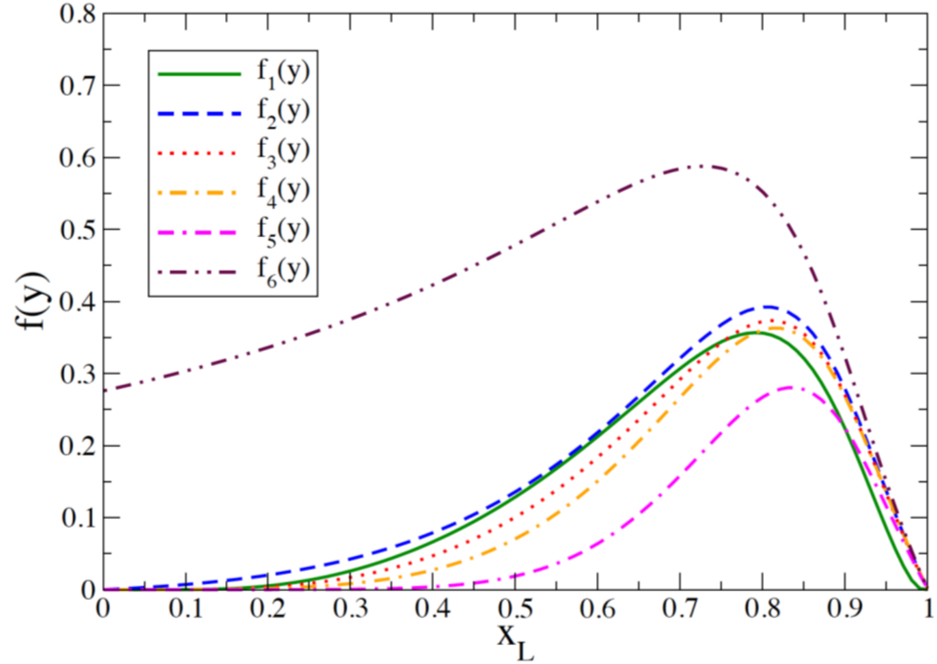

Flux factor

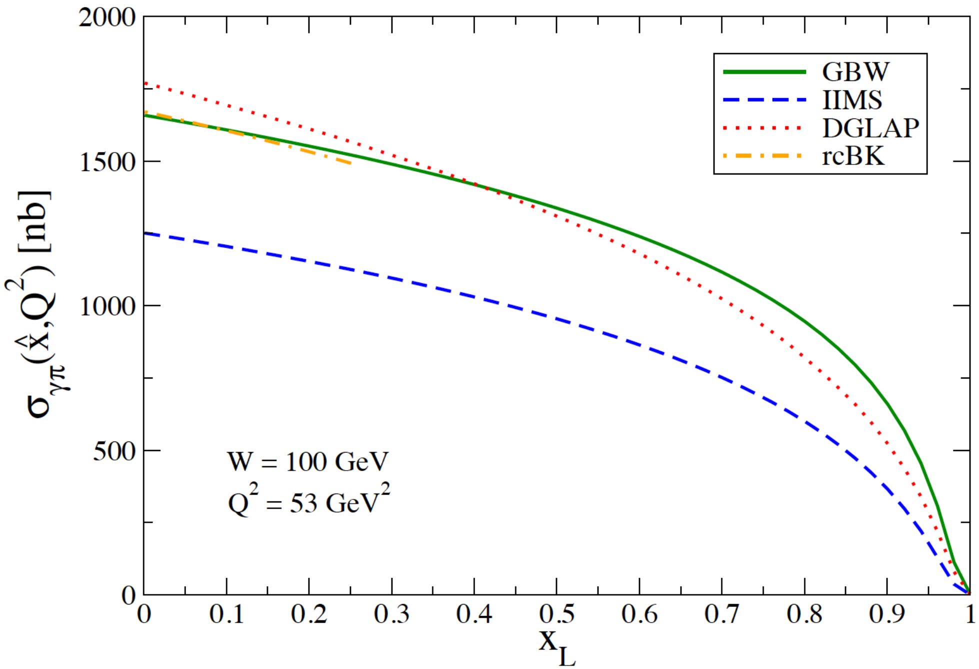

Dipole cross section

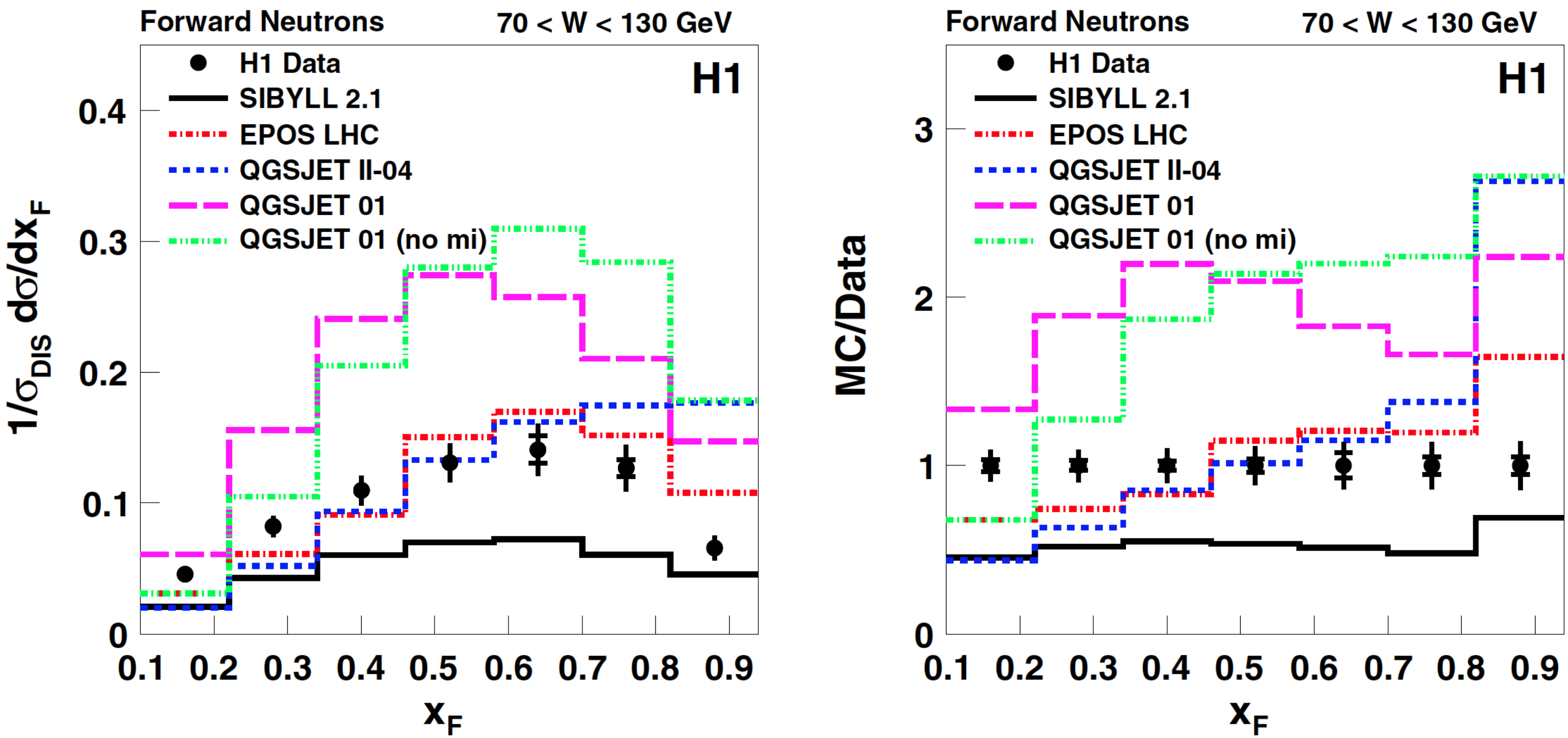

Forward Neutrons
70 < W < 130 GeV
H1 Data
SIBYLL 2.1
EPOS LHC
QGSJET II-04
QGSJET 01
QGSJET 01 (no mi)
H1
$1/\sigma_{DIS}\, d\sigma/dx_F$
0
0.1
0.2
0.3
0.4
0.1 0.2 0.3 0.4 0.5 0.6 0.7 0.8 0.9
x_F
Forward Neutrons
70 < W < 130 GeV
H1 Data
SIBYLL 2.1
EPOS LHC
QGSJET II-04
QGSJET 01
QGSJET 01 (no mi)
H1
MC/Data
0
1
2
3
0.1 0.2 0.3 0.4 0.5 0.6 0.7 0.8 0.9
x_F

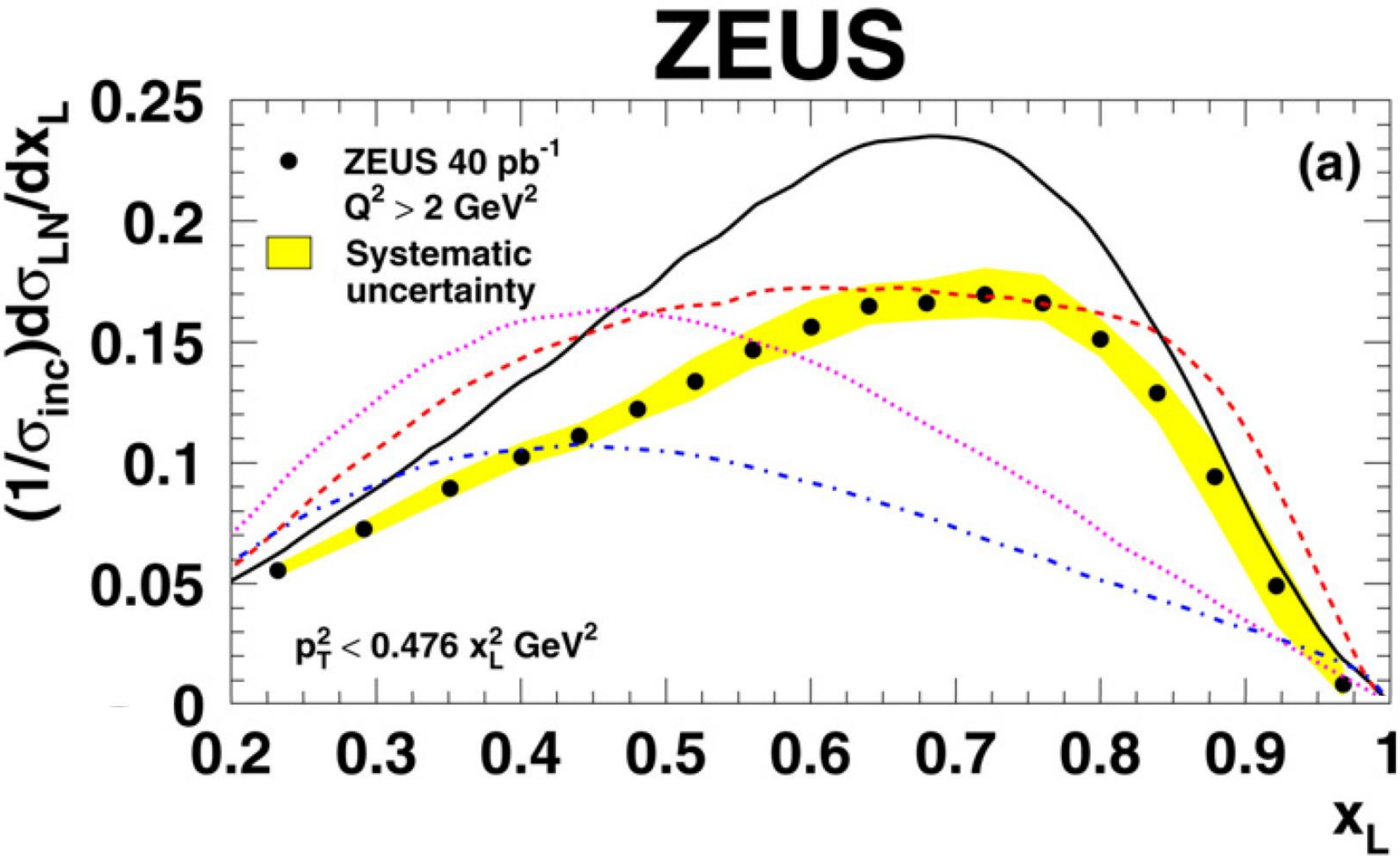

ZEUS
(a)
ZEUS 40 pb^{-1}
$Q^2 > 2$ GeV^2
Systematic uncertainty
$p_T^2 < 0.476\ x_L^2$ GeV^2
$(1/\sigma_{inc})d\sigma_{LN}/dx_L$
x_L
0
0.05
0.1
0.15
0.2
0.25
0.2
0.3
0.4
0.5
0.6
0.7
0.8
0.9
1

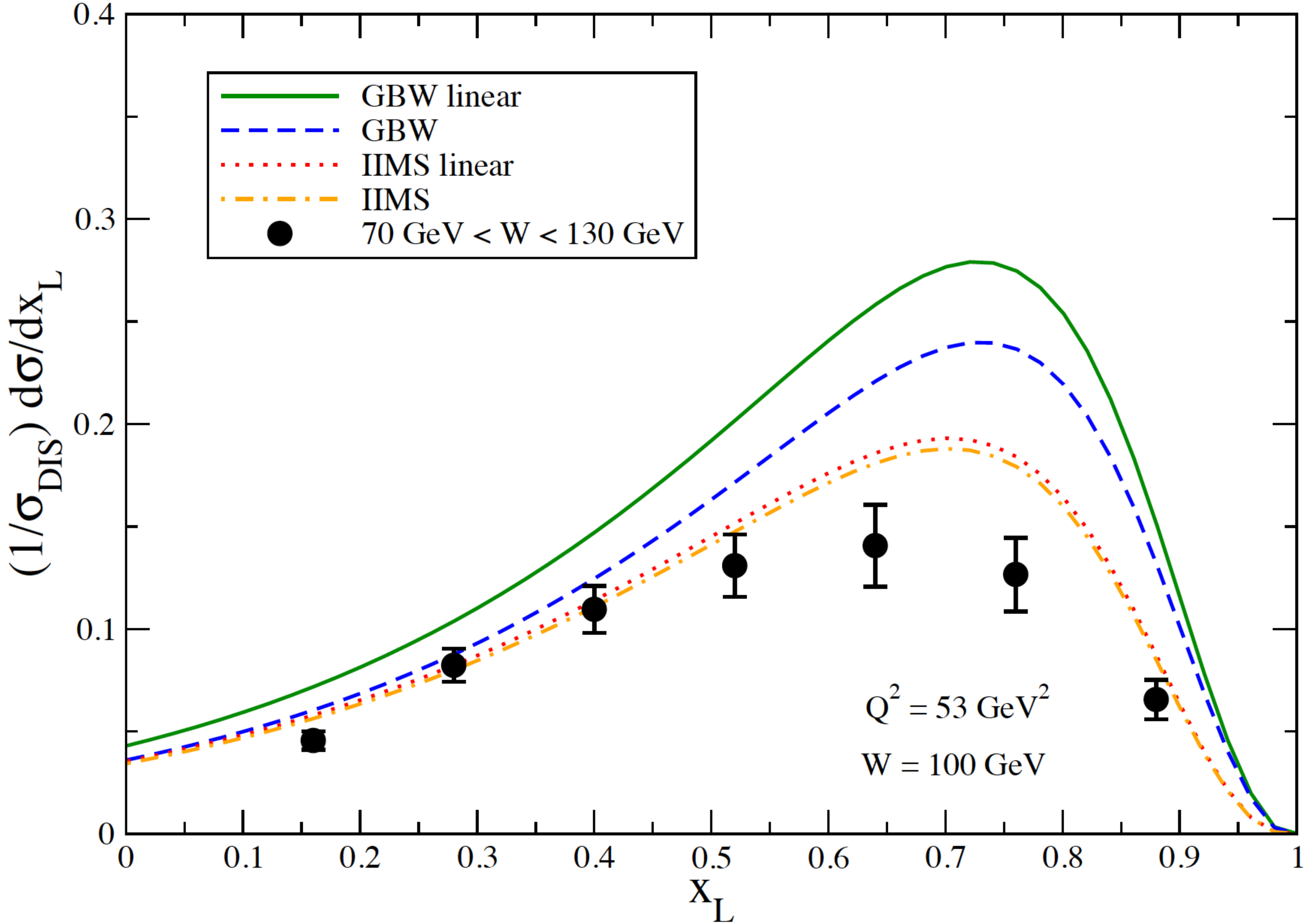

GBW linear
GBW
IIMS linear
IIMS
70 GeV < W < 130 GeV
$Q^2 = 53\ \mathrm{GeV}^2$
$W = 100\ \mathrm{GeV}$
$(1/\sigma_{DIS})\ d\sigma/dx_L$
x_L
0
0.1
0.2
0.3
0.4
0.5
0.6
0.7
0.8
0.9
1

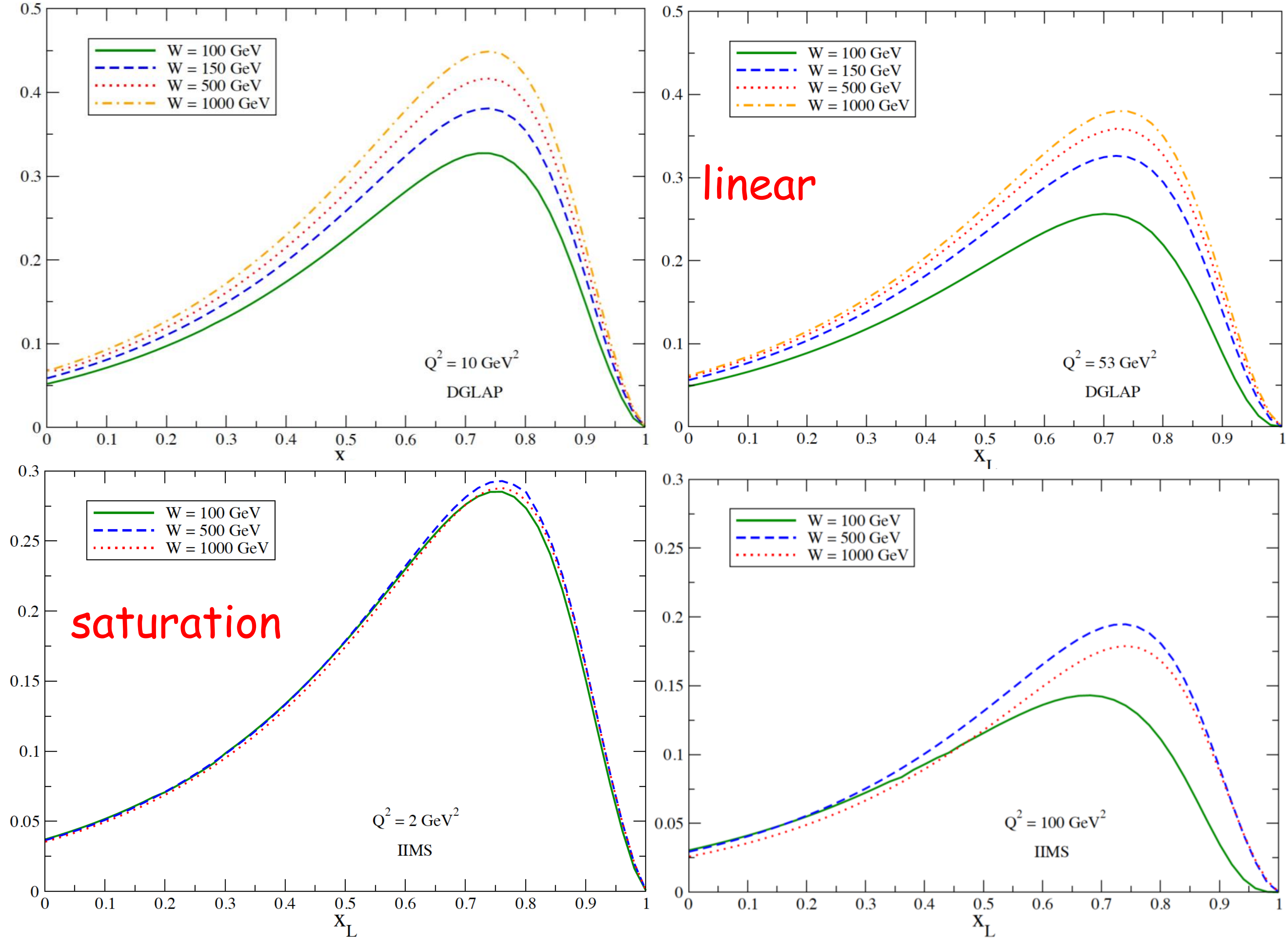

W = 100 GeV
W = 150 GeV
W = 500 GeV
W = 1000 GeV
Q² = 10 GeV²
DGLAP
x
linear
W = 100 GeV
W = 150 GeV
W = 500 GeV
W = 1000 GeV
Q² = 53 GeV²
DGLAP
x_L
saturation
W = 100 GeV
W = 500 GeV
W = 1000 GeV
Q² = 2 GeV²
IIMS
x_L
W = 100 GeV
W = 500 GeV
W = 1000 GeV
Q² = 100 GeV²
IIMS
x_L

that is hard for small momentum transfers and soft for large momentum transfers.

Other isovector meson exchanges, such as the ρ or a_2, can also contribute to direct neutron production. Recent theoretical studies of neutron production in ep collisions show that processes other than direct pion exchange are expected to contribute $\lesssim 25\%$ of neutron production [33,60,61,67]. These backgrounds to OPE, which increase the rate of neutron production in the FNC phase space, are offset by absorptive rescattering of the neutron, which decreases the rate by approximately the amount of the increase [68, 69]. Also absorptive rescattering preferentially removes neutrons with larger p_{T}, increasing the pion contribution relative to the ρ and a_2. Therefore these effects are also neglected in the present analysis.

10.1 Competing processes to OPE

Several processes which compete with pion exchange as the mechanism for leading neutron production were ignored in Eq. (16), namely:

- diffractive dissociation in which the dissociated system decays to a state including a neutron

Diffractively produced events can be selected by requiring the presence of a large rapidity gap in the hadronic final state. For such events, the mass of the dissociated proton system is restricted to low values, $M_{\mathrm{N}} \lesssim 4$ GeV.

An event is said to have a large rapidity gap (LRG) in the ZEUS detector if the pseudorapidity of the most-forward energy deposit with energy greater than 400 MeV (η_{max}) is less than 1.8 [64]. Figure 17(a) shows the η_{max} distributions for both the neutron-tagged and inclusive DIS samples, where the latter has been normalised to the neutron-tagged sample for $\eta_{\mathrm{max}} > 1.8$. For both $\eta_{\mathrm{max}} < 1.8$ and $\eta_{\mathrm{max}} > 1.8$, the shape of the neutron-tagged distribution is similar to that of the inclusive distribution; however, there are relatively fewer LRG events in the neutron-tagged sample. The LRG events represent only 4% of the total number of DIS events with neutrons in the measured kinematic region, but are 7% of the total number of DIS events. A reduction in the fraction of LRG events with a final-state neutron is expected since only proton diffractive dissociation or diffractive meson exchange (the Deck effect [65]) can contribute.

To investigate a possible x_L-dependence of the contribution of diffractive events, Fig. 17(b) shows the ratio, R_{LRG}, of the neutron-tagged DIS events, selected by the LRG criterion, to all neutron-tagged DIS events, as a function of x_L. The rise by a factor of three over the x_L range shows that the LRG neutron-tagged events have a harder neutron energy spectrum than that of the inclusive neutron-tagged sample. It is clear that diffractive events are not a major source of leading neutrons at any value of x_L. For the region $0.64 < x_L < 0.82$, R_{LRG} is 0.039 ± 0.001 (*stat.*);

- ρ and a_2 exchange

  Theoretical studies of neutron production in ep collisions [18, 53] suggest that isovector exchanges other than the pion contribute less than 10% to neutron production at $x_L = 0.73$ and for the p_T range of the present data. This is quite different than for leading proton production, where isoscalar Regge exchange provides the dominant contribution [2, 19];

- isovector exchange leading to Δ production

  The $p \to \Delta(1236)$ transition, formed by π, ρ and a_2 exchange, can also contribute to neutron production [18, 53, 66–68]. In this case, the neutron, which comes from the decay $\Delta^0 \to n\pi^0$ or $\Delta^+ \to n\pi^+$, no longer has an energy determined by the energy of the exchanged meson. The neutron energy spectrum peaks near $x_L \approx 0.5$ and extends only to $x_L \approx 0.7$ [19]. It thus gives a small contribution in the $0.64 < x_L < 0.82$ bin. A comparison of the data on $p \to n$ and $p \to \Delta^{++}$ [69–72] in charge-exchange reactions at Fermilab indicates that only about 6% of the forward neutrons come from the Δ channel. This observation agrees with theoretical estimates of the $\Delta\pi$ contribution to the Fock state of the proton, which is approximately half that of $n\pi$ [53, 66]. A calculation [67] shows that the contribution of ρ/a_2 exchange, plus the Δ contribution, to the hadronic charge-exchange reaction $pp \to Xn$ could be as high as 30%. Since no analogous calculation exists for DIS, this only provides an indication of a possible background to the neutron production discussed in this paper;

- models other than one-particle exchange

  Monte Carlo studies, using standard DIS generators, show [1] that these processes have a rate of neutron production a factor of three lower than the data and produce a neutron energy spectrum with the wrong shape, peaking at values of x_L below 0.3.

In summary, the expectation for the processes listed above at $\langle x_L \rangle = 0.73$ and $\langle {p_T}^2 \rangle = 0.08$ GeV^2 is that they contribute of the order of 20% of the leading neutron production. This estimate can be checked using the measured neutron-energy spectrum. The OPE fit to the differential cross-section $d\sigma/dx_L$ shown in Fig. 8(a) suggests that, at $x_L = 0.73$, the residual background to OPE is $\lesssim 10\%$, in reasonable accord with the studies discussed above.

Gluon saturation

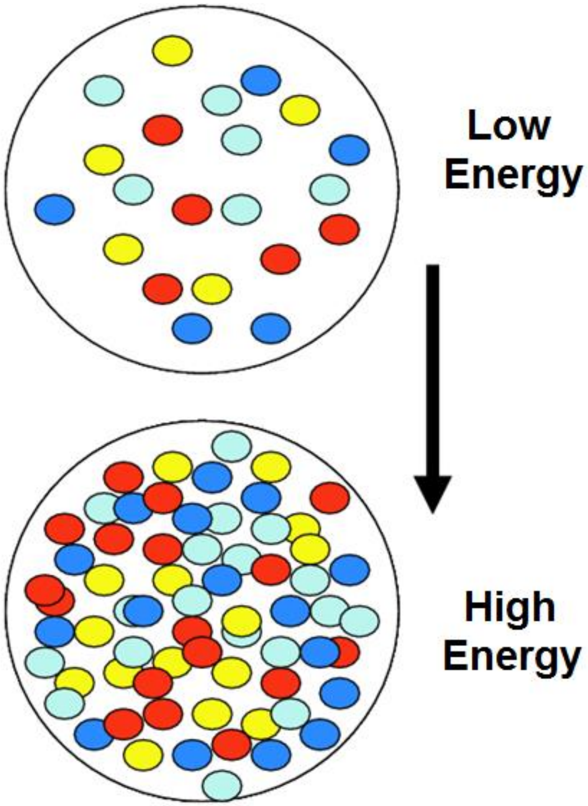

High energies
large number of gluons
gluon recombination

$$g\,g \rightarrow g$$

Gluon recombination at very small **x** tames the growth of the gluon distribution

Implementation: color dipole approach

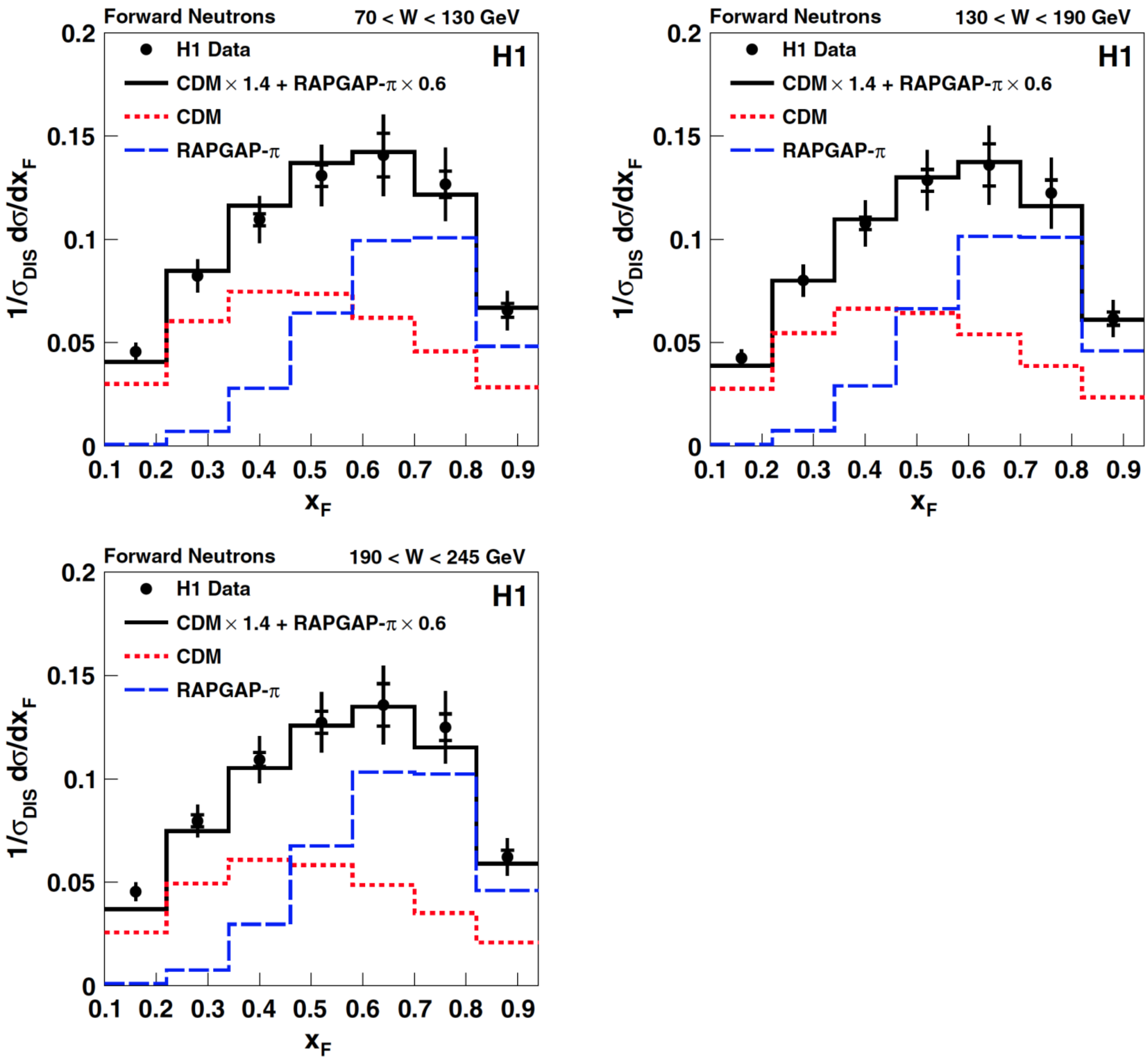
Forward Neutrons
70 < W < 130 GeV
130 < W < 190 GeV
190 < W < 245 GeV
H1
H1 Data
CDM × 1.4 + RAPGAP-π × 0.6
CDM
RAPGAP-π
1/σ_DIS dσ/dx_F
x_F
0
0.05
0.1
0.15
0.2
0.1 0.2 0.3 0.4 0.5 0.6 0.7 0.8 0.9

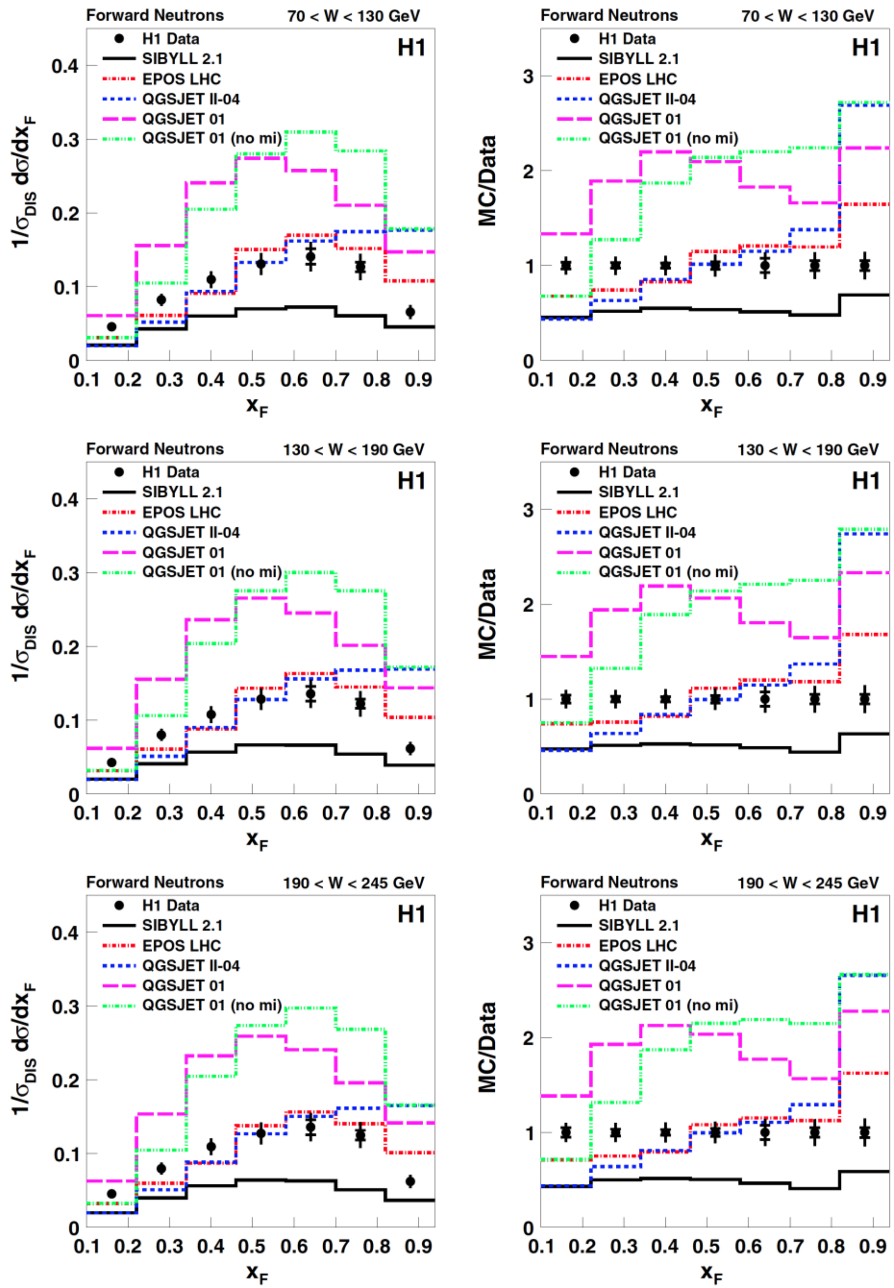

Forward Neutrons
70 < W < 130 GeV
H1
H1 Data
SIBYLL 2.1
EPOS LHC
QGSJET II-04
QGSJET 01
QGSJET 01 (no mi)
1/σ_DIS dσ/dx_F
x_F
Forward Neutrons
70 < W < 130 GeV
H1
H1 Data
SIBYLL 2.1
EPOS LHC
QGSJET II-04
QGSJET 01
QGSJET 01 (no mi)
MC/Data
x_F
Forward Neutrons
130 < W < 190 GeV
H1
H1 Data
SIBYLL 2.1
EPOS LHC
QGSJET II-04
QGSJET 01
QGSJET 01 (no mi)
1/σ_DIS dσ/dx_F
x_F
Forward Neutrons
130 < W < 190 GeV
H1
H1 Data
SIBYLL 2.1
EPOS LHC
QGSJET II-04
QGSJET 01
QGSJET 01 (no mi)
MC/Data
x_F
Forward Neutrons
190 < W < 245 GeV
H1
H1 Data
SIBYLL 2.1
EPOS LHC
QGSJET II-04
QGSJET 01
QGSJET 01 (no mi)
1/σ_DIS dσ/dx_F
x_F
Forward Neutrons
190 < W < 245 GeV
H1
H1 Data
SIBYLL 2.1
EPOS LHC
QGSJET II-04
QGSJET 01
QGSJET 01 (no mi)
MC/Data
x_F

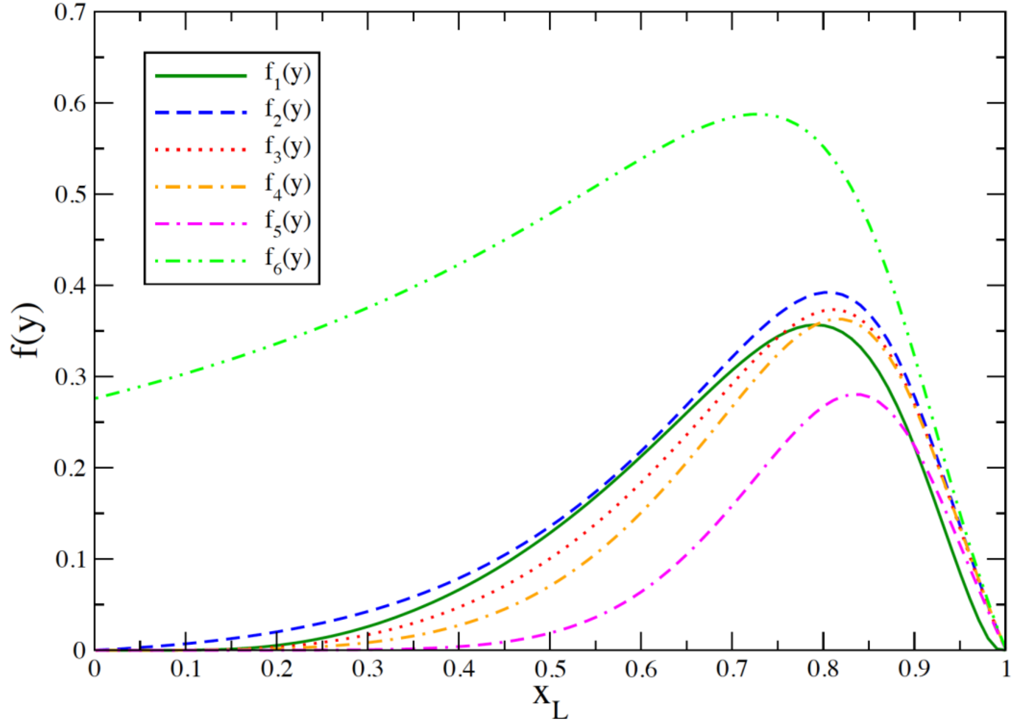

Flux factor

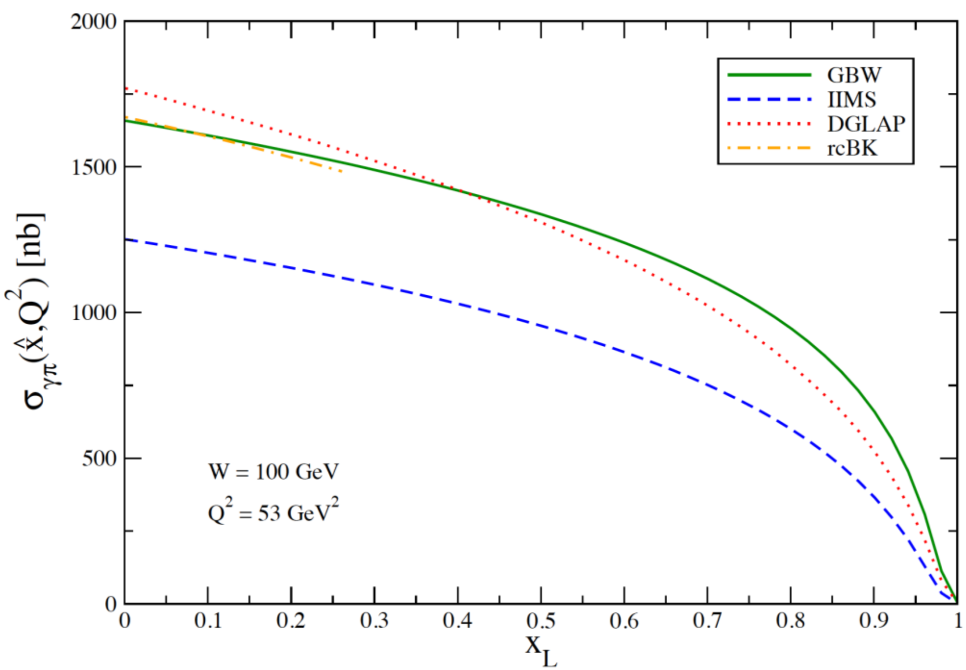

Dipole cross section

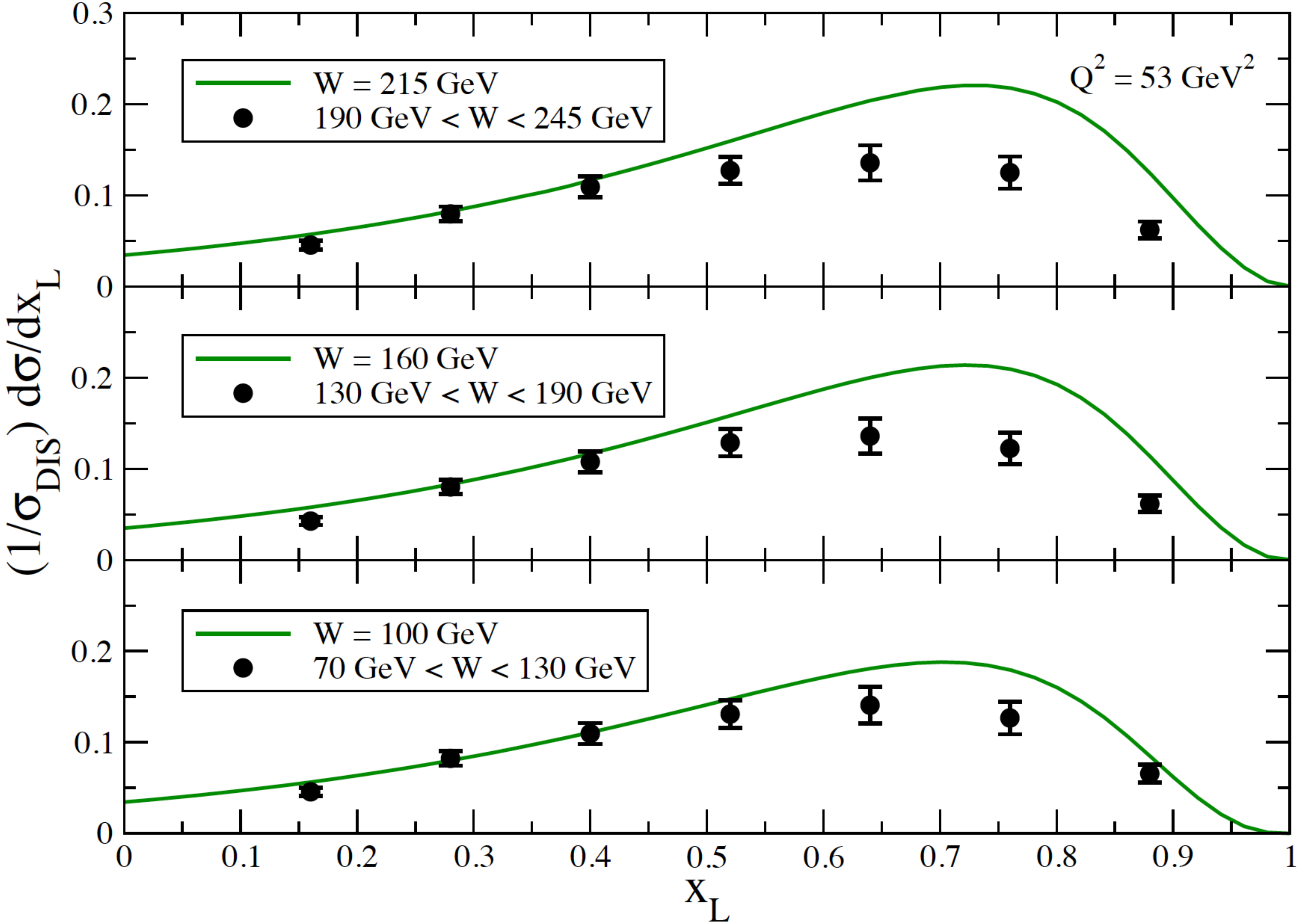

W = 215 GeV
190 GeV < W < 245 GeV
$Q^2 = 53$ GeV^2
W = 160 GeV
130 GeV < W < 190 GeV
W = 100 GeV
70 GeV < W < 130 GeV
$(1/\sigma_{DIS})\, d\sigma/dx_L$
x_L
0
0.1
0.2
0.3
0.4
0.5
0.6
0.7
0.8
0.9
1

$$\hat{x} = \frac{Q^2 + m_f^2}{\hat{W}^2 + Q^2} = \frac{Q^2 + m_f^2}{(1 - x_L)W^2 + Q^2}$$

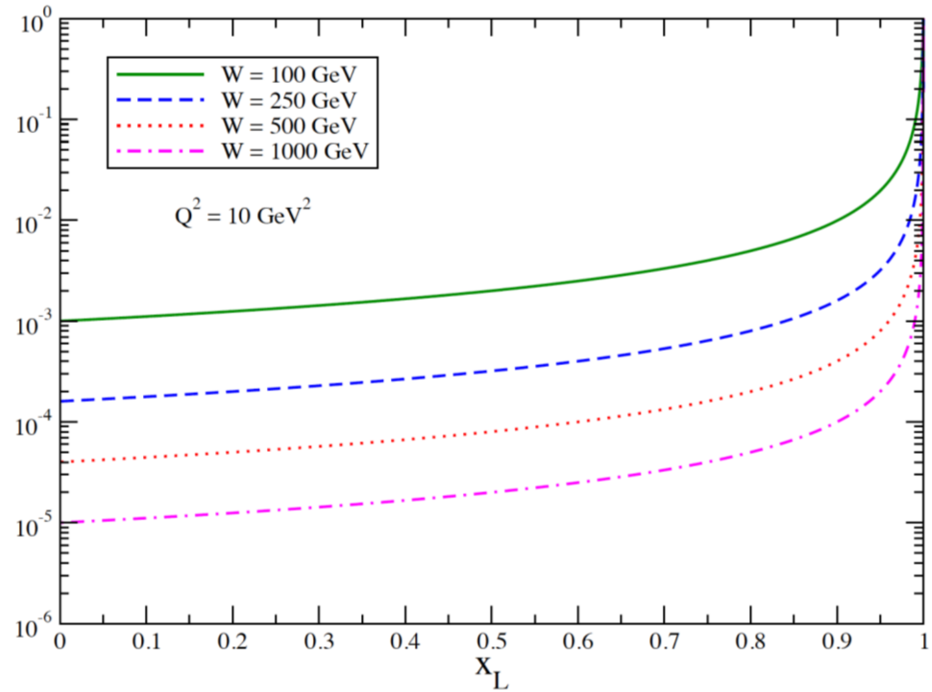

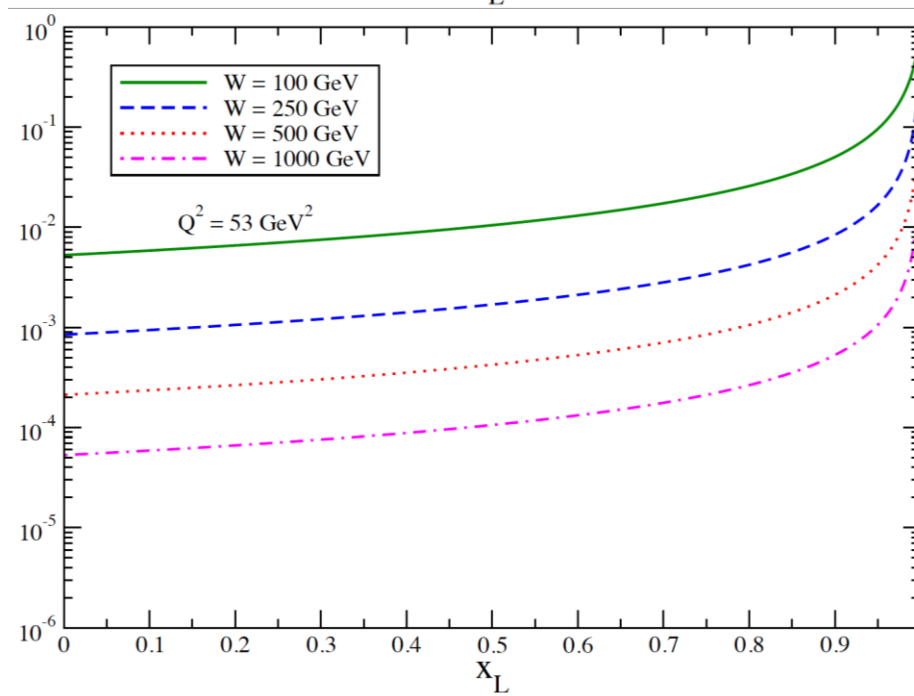

Leading neutron production can be low x physics !

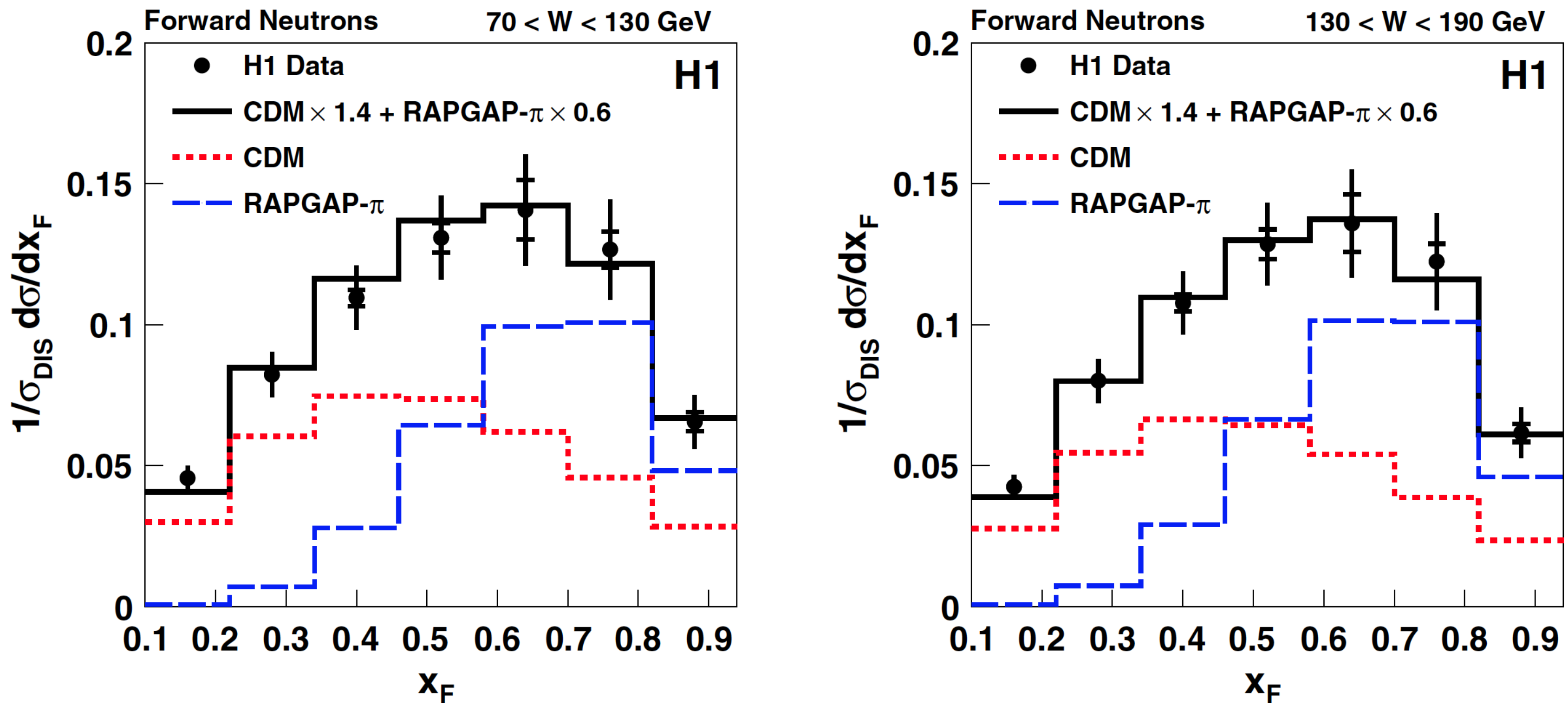

Forward Neutrons
70 < W < 130 GeV
H1
H1 Data
CDM × 1.4 + RAPGAP-π × 0.6
CDM
RAPGAP-π
$1/\sigma_{DIS}\ d\sigma/dx_F$
x_F
0.2
0.15
0.1
0.05
0
0.1 0.2 0.3 0.4 0.5 0.6 0.7 0.8 0.9
Forward Neutrons
130 < W < 190 GeV
H1
H1 Data
CDM × 1.4 + RAPGAP-π × 0.6
CDM
RAPGAP-π
$1/\sigma_{DIS}\ d\sigma/dx_F$
x_F
0.2
0.15
0.1
0.05
0
0.1 0.2 0.3 0.4 0.5 0.6 0.7 0.8 0.9